Prayogik Rasayan

Terpenoids in Early 21st Century: From Renewable Functional Nano-entities to Advanced Materials

Braja Gopal Bag,* Subhajit Das, Sk Nurul Hasan, Abir Chandan Barai, Subrata Ghorai, Saikat K. Panja, Chhabi Garai, Sanjit Santra

Department of Chemistry and Chemical Technology, Vidyasagar University Midnapore 721102, West Bengal, India,
Email: brajagb@gmail.com

Received: November 24, 2017| Accepted: December 22, 2017 | Published online: January 02, 2018

Abstract

Plant metabolites can serve as renewable chemicals for the development of a sustainable society. Terpenoids are the major component of over 500,000 plant secondary metabolites reported till date. Monoterpenoid (C10) to tetraterpenoid (C40) all the terpenoid have recently been shown to have nanometric lengths. Studies on the self-assembly of terpenoids, have drawn the attention of scientific community in recent years due to many of its potential and realized applications in medicine, drug delivery, pollutant capture, metal nanoparticle hybrid material, selective damage of cancer cells, etc. In this review, we have discussed the isolation of seven terpenoids from plants and their self-assembly properties in different liquids, even without functional transformation. The utilization of the resulting supramolecular architectures such as vesicles, spheres, flowers and fibrillar networks of nano- to micro-meter dimensions and gels have also been discussed paving the way for a green, renewable and sustainable world.

Keywords: Terpenoids, self-assembly, renewable, drug delivery, soft-material

1. Introduction

Terpenoids are a large and structurally diverse group of natural products containing multiple of C5 (isoprene) units. They are categorized by the number of C5 units as: hemi- (one C5 unit), mono- (C10; two C5 units), sesqui- (C15; three C5 units), di- (C20; four C5 units), sester- (C25; five C5 units), tri- (C30; six C5 units), sesquarterpenes (C35; seven C5 units) and tetraterpenes (C40; eight C5 units). Isolation of over 50,000 terpenoids from plants has been reported so far and these are the major components of over 500,000 plant secondary metabolites reported till date. These plant secondary metabolites play an important role in self-defenses against harmful organisms, coloring fruits and petals, attracting pollinators, communicating with neighboring plants, etc.[12] In recent years, there has been a resurgence on the utilization of plant metabolites as the source of raw materials in organic chemistry research instead of the petroleum based chemicals because such a strategy aims at the development of a sustainable society.[3,4,5,6,7,8,9,10]

Nanoscience and nanotechnology deal with the investigation of the properties of atomic, molecular or supramolecular aggregates consisting of at least one of their dimensions in the nano-metric range (usually within 1 – 100 nm).[11,12,13,14,15] Since 1980s, syntheses of different inorganic nanoparticles including elemental metals, metal oxides, metal sulfides, metal selenides, and metal tellurides have been reported with excellent control over size and shape.[16,17] Initial investigations were mainly focused on the exploration of the quantum size effects of such materials. The applications of inorganic nanomaterials initially centered on physics, optics, and engineering and then slowly expanded to biology and catalysis[18,19] Some inorganic nanomaterials have found applications as biochemical sensors, contrast agents in cellular or tissue imaging, drug delivery vehicles and therapeutics.[20] Nucleic acids, proteins, polysaccharides, lipids are some of the mostly studied naturally occurring nano-sized building blocks in bioorganic and supramolecular chemistry.[21,22,23,24,25,26,27] Since Ruzicka's proposal of the biogenetic isoprene rule that 'all the triterpenoids are biosynthesized from the common precursor squalene, the triterpenoids containing 30C have been recognized as a very special class of natural products.[28] Investigations carried out during the last six decades have not only supported his hypothesis but also have provided a tool for the structural establishment of newer triterpenoids. Recent computational results have shown that all these C30 plant metabolites have lengths within 1-3 nm. Thus triterenoids can serve as renewable functional nano-entities with varied rigid and flexible lengths.[29] In this review we show that all the terpenoids namely mono-, di-, tri- and tetra-terpenoids are nano-sized molecules having a wide range of skeletal diversities and functional groups. Spontaneous self-assembly of the terpenoids in different liquids yielding vesicles, fibers, spheres, tubules, flowers have been discussed. Utilization of the self-assemblies for the entrapment of fluorophores including anticancer drugs doxorubicin, removal of toxic chemicals, generation of hybrid materials, recyclable heterogeneous catalyst have also been discussed.

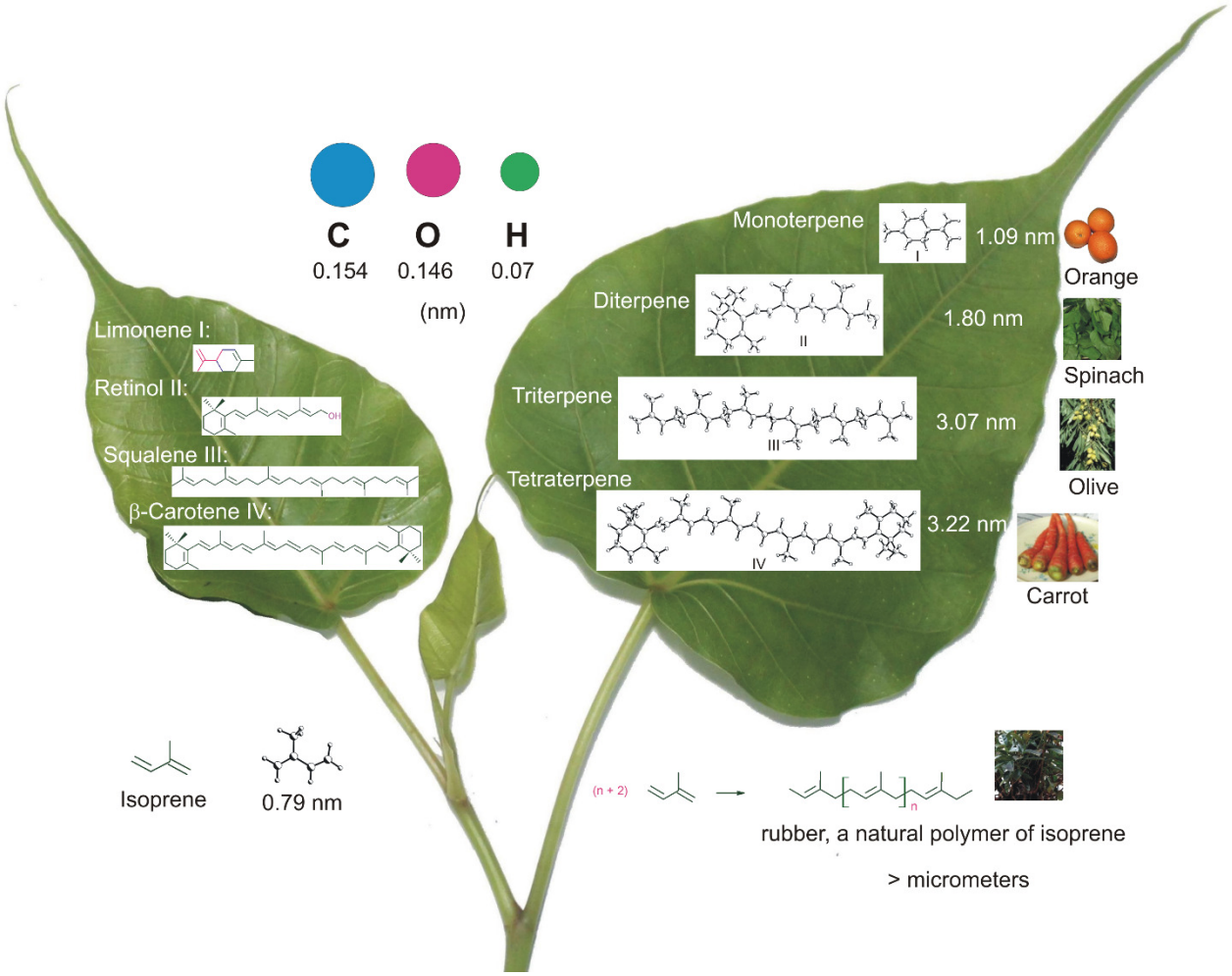

Figure 1: Structures of representative terpenoids, their energy minimized structures and computed lengths in nanometer (nm) unit with leaves of *Ficus religiosa* in the background. Left leaf: structures of limonene I, retinol II, squalene III, □-carotene IV; right leaf: energy minimized structures of I-IV along with their computed lengths. Common natural sources of the the representative terpenoids are shown on the right.

2. Terpenoids as renewable functional nano-entities

Terpenoids having acyclic and cyclic structures with over 100 different skeletons have been isolated from nature. Functional terpenoids having several centers of chirality and functional groups such as hydroxyl, carboxyl or aldehyde groups are very common. Computations carried out by us on representative mono-, di, tri-, and tetra-terpenoids by molecular mechanics calculation using Allinger's MMX algorithm have shown that all the terpenoids are of nano-metric lengths (Figure. 1).[30] For example, the molecular length of d-limonene, a monocyclic mono-terpene is 1.09 nm. The very strong smell of orange is due to the presence of this chiral monoterpene d-limonene. Retinol, a diterpenoid extractable from spinach, is 1.80 nm long. Retinol along with the other components of vitamin A such as retinal, retinoic acid, both of which are also nano-sized molecules, play a critical role in maintaining healthy vision, neurological function and healthy skin.

Triterpenoids are the 30-carbon subset of the terpenoids. These can exist either in acyclic or mono- to pentacyclic forms having distinct skeletal diversities. Detailed molecular mechanics calculation with sixty representative triterpenoids using Allinger's MMX algorithm and conformation search using MacroModel and Monte Carlo technique with the MM3 force-field revealed that all the triterpenoids have lengths exceeding 1 nm[31,32] For acyclic and alicyclic triterpenoids, the nanometric lengths are maintained even after folding. The acyclic triterpenoid squalene is 2.73 nm long. For mono-, bi-, tri-, tetra- and pentacyclic triterpenoids, the molecular lengths gradually decreased and became completely rigidified in pentacyclic triterpenoids with a length of the rigid backbone of 1.2 nm.

The tetra-terpenoid □-carotene is 3.22 nm long. It is a red-orange pigment present in different plants and fruits especially carrot. This serves as the provitamin A and once consumed, one molecule of β-carotene is converted to two molecules of vitamin A.

The isoprene unit can undergo polymerization to yield the natural rubber, a biopolymer. The lengths of such biopolymers can be over micrometers.

Thus all the terpenoids are nano-sized molecules having wide skeletal and functional group diversities. As the terpenoids are extractable from different parts of the plants such as leaves, barks, flowers, fruits, roots, heavy-woods etc., these are an attractive choice for the use of them as renewable functional nano-entities in various facets of nanoscience and nanotechnology.

3. Self-assembly of terpenoids

Self-assembly is a process by which individual components spontaneously form an organized structure via specific local interactions among the components without external direction. Spontaneous hierarchical self-assembly of molecules in liquids yielding supramolecular structures of nano- to micro-meter dimensions has been an area of intense research in recent years for an improved understanding of different supramolecular architectures and because of their many potential and realized technological applications.[33,34,35,36] Self-assembly of different classes of naturally occurring compounds such as sugars,[37] amino acids,[38] fatty acids,[39] sophorolipids,[40] steroids etc. have been reported in the recent literature.[41] But, in spite of the abundance of over 50,000 of naturally occurring terpenoids,[42] there was no report on the self-assembly of terpenoids till recently.[43] Computational results showed that all the naturally occurring mono-, di-, tri- and tetra-terpenoids have nanometric lengths.

Among various plant secondary metabolites, terpenoids are of special significance for the study of their self-assembly properties in different liquids because of the following reasons: (i) wide range of skeletal diversities provide lypophilic backbone of varied rigid and flexible lengths, (ii) the presence of one or more hydroxyl and/or carboxyl groups make them useful as functional nano-entities, (iii) the in-built chirality with upto ten chiral centers makes them useful as chiral building blocks, (iv) the amphiphilic nature of the functional terpenoids provides promising self-assembly properties even without derivatization, (v) easy transformation of the functional groups allows the generation of libraries of derivatives. As the functional terpenoids were extractable from plants, we extracted seven terpenoids from different plants and studied their self-assembly properties in different liquids. The functional terpenoids with diversified structures along with varied number of hydroxyl and carboxyl groups spontaneously self-assembled in different liquids even without derivatization yielding nanoarchitectures such as vesicles, fibers, flowers, spheres, tubules, etc. The self-assemblies have been utilized for the entrapment and release of drug molecules, removal of toxic chemicals, thermochromic materials, generation of gel-

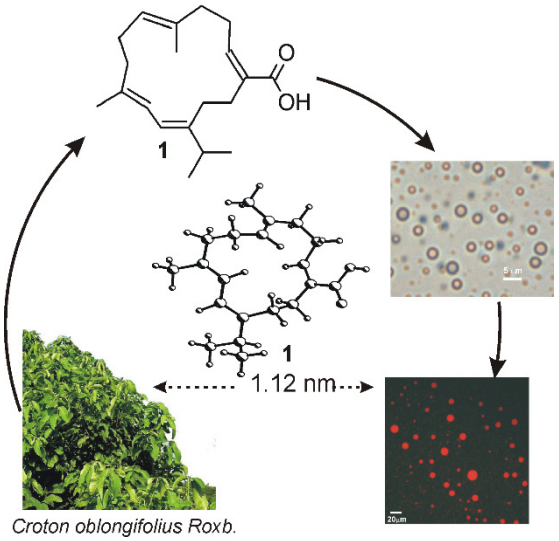

Figure 2. Schematic representation of self-assembly of crotocembraneic acid **1** extractable from *Croton oblongifolius* Roxb yielding vesicular self-assemblies and its use in drug entrapment studies (centre: energy minimized structure of **1**). Reprinted (adapted) with permission from ref. 45 Copyright 2017 John Wiley and Sons.

metal nanoparticle hybrid material, heterogeneous catalysis, etc.

3.1 Self-assembly of a macrocyclic diterpenoid crotocembraneic acid 1

The diterpenoids are C20 subset of terpenoids derived from geranylgeranyl. They have a highly diverse skeletal diversities containing acyclic to mono-, bi- and tricyclic structures with several centers of chirality having hydroxyl, carboxyl, aldehyde and phenolic groups as common functional groups.[44] Computations carried out by us have revealed that all the diterpenoids are of nanometric lengths. In the course

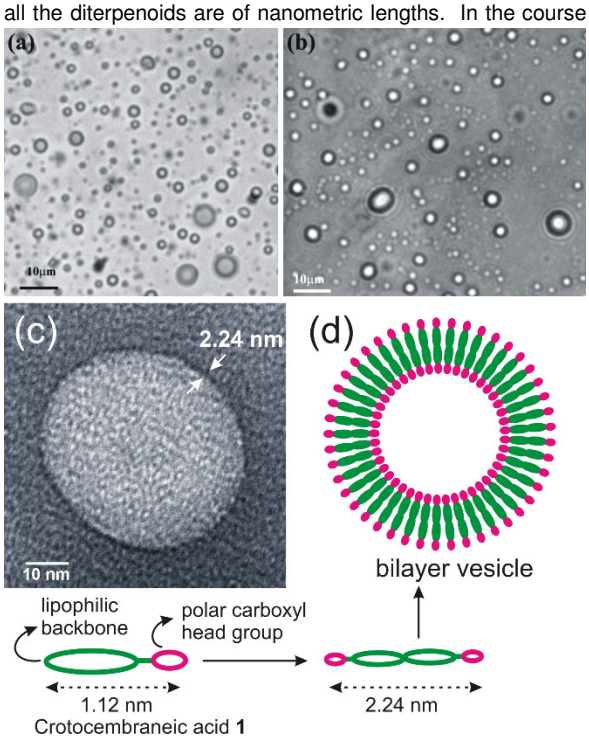

Figure 3. (a,b) Optical micrographs of Crotocembraneic acid 1 in (a) ethanol-water (2% w/v) (b) DMSO-water (2% w/v), (c) HRTEM of dried self-assemblies of **1** prepared from its colloidal suspension in ethanol-water (2:1 v/v), (d) schematic representation of the formation of bilayer membrane yielding vesicular self-assembly of **1**. Reprinted (adapted) with permission from ref. 45 Copyright 2017 John Wiley and Sons.

of our investigations, we have successfully isolated a macrocyclic diterpenoid crotocembraneic acid **1** (Figure. 2), from the leaves of *Croton oblongifolius* Roxb. It has a unique 14-membered macrocyclic structure having four double bonds within the macrocycle; two double bonds in the conjugated position and two double bonds in the non-conjugated positions. The molecular length obtained by molecular mechanics calculation was 1.12 nm. The molecule has an amphiphilic nature with the carboxyl group forming a polar 'head' and the macrocycle forming a highly hydrophobic 'tail'. Thus crotocembraneic acid **1** turned out to be a unique diterpenoid for the study of its self-assembly properties in various liquids.[45]Crotocembraneic acid **1** was extracted from the leaves of *Croton oblongifolius* Roxb by following an optimized procedure developed in our laboratory as a low melting solid.[46,47] The compound was highly soluble in polar solvents such as ethanol, DMSO, DMF and formed suspensions in aqueous binary solvent mixtures. Polydisperse spherical self-assemblies with an average size of 200 nm was observed in a colloidal suspension of **1** (1.18% w/v) in ethanol-water (2:1 v/v) when examined by Dynamic Light Scattering (DLS) studies. An increase in the average size of the self-assemblies to 465 nm and 523 nm were observed on increasing the concentration of **1** to 1.6% w/v and 2.2% w/v respectively, with a small fraction of the assemblies having micrometer diameters.

Thorough analysis of the self-assemblies by optical microscopy in their native state in binary solvent mixtures such as ethanol-water (2:1 v/v), DMSO-water (2:1 v/v) and DMF-water (2:1 v/v) indicated micro-sized spherical self-assemblies of average diameter of 2 □m (Figure. 3).

Detailed investigations of the morphology of dried self-assemblies by atomic force microscopy (AFM) (Figure. 4), scanning electron microscopy (SEM) and high resolution transmission electron microscopy (HRTEM, Figure. 3) indicated the vesicular nature of the self-assemblies. A distinct periphery of thickness 2.24 nm was also observed by HRTEM. The molecular length being 1.12 nm, a bilayer vesicular self-assembly is supported (Figure. 3c-d). Such a bilayer vesicular self-assembly is also supported by x-ray diffraction studies.

As the vesicular self-assemblies were smaller than 10 □m, considering their importance in prospective drug delivery applications through blood capillaries,[48] we tested the entrapment of various cationic and anionic fluorophores including an anticancer drug. Interestingly, the cationic fluorophore rhodamine B (Rho-B), anionic fluorophore 5,6-carboxyfluorescein (CF) and an well known anticancer drug doxorubicin could be entrapped inside the vesicular self-assemblies (Figure. 5). Availability of the diterpenoids in plenty from nature and the simplicity of the methods of self-assembly and drug entrapment described here makes our strategy applicable to other naturally occurring diterpenoids.

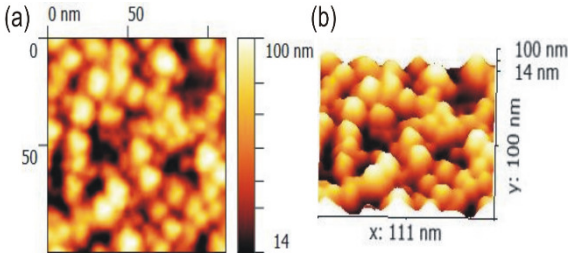

Figure 4. (a,b) AFM images (2D and 3D respectively) of spherical self-assemblies formed from **1** (0.28% w/v) in DMSO-water (2:1 v/v). Reprinted (adapted) with permission from ref. 45 Copyright 2017 John Wiley and Sons.

.

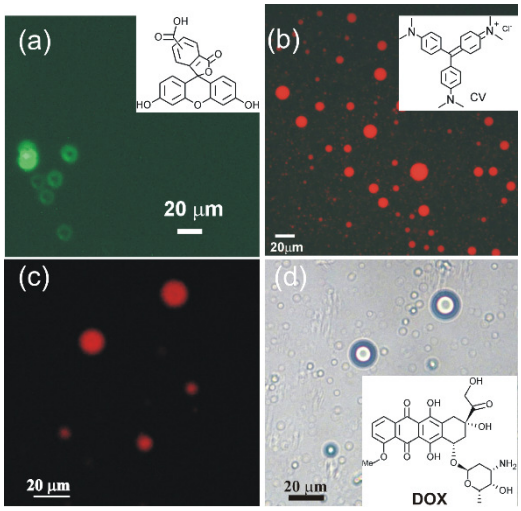

Figure 5. Epifluorescent microscopy images of (a,b) self-assembled **1** (26.0 mM) in DMSO-water (2:1 v/v): (a) containing CF (0.26 mM); (b) containing crystal violet (0.463 mM), (c,d) self-assembled **1** (46.32 mM) in DMSO-water (2:1 v/v) containing doxorubicin (0.46 mM); (a,b,c) fluorescent images, (d) bright-field image. Reprinted (adapted) with permission from ref. 45 Copyright 2017 John Wiley and Sons.

Table 1. Gelation test results of betulinic acid **2**[a]

Entry[a]	Solvent	State3[b]	MGC[c]	T_{gel} °C
1	Benzene	G	2.50	>85
2	Toluene	G	1.43	70-72
3	o-xylene	G	1.06	75-78
4	m-xylene	G	2.50	>90
5	p-xylene	G	5.00	>90
6	Mesitylene	G	2.04	74-76
7	Bromo benzene	G	0.54	46-47
8	Chloro benzene	G	2.57	>85
9	o-dichloro benzene	G	0.41	44-46
10	Nitrobenzene	G	0.90	62-65
11	p-methoxy benzaldehyde	G	3.5	64-66
12	Methanol	CS	1.25	-
13	Ethanol	CS	3.4	-
14	n-Propanol	G	10.0	76-77
15	n-Butanol	G	10.0	>90
16	n-Pentanol	G	10.0	>90
17	n-hexanol	G	10.0	78-79
18	n-heptanol	G	10.0	80-81
19	n-octanol	G	10.0	>90
20	Chloroform	CS	2.65	-
21	Carbontetrachloride	G	0.48	61-63
22	1,1,2,2-Tetrachloroethane	G	2.08	54-55

[a] Gelation tests were carried out with a maximum concentration of 10% w/v. [b] G = gel, CS = Colloidal suspension; [c] MGC is the minimum gelator concentration (% w/v) in which the gel is formed at room temperature.

3.2 Self-assembly of betulinic acid 2

Betulinic acid 2 (Figure. 6d), a 1.31 nm long 6-6-6-6-5 pentacyclic monohydroxy triterpenic acid is extractable from the bark of Ziziphus jujube. The molecule has a hydroxyl attached at the 'A' ring and the carboxyl group attached at ring junction of the trans-fused 'D' and 'E' rings having a 0.97 nm rigid and lyphophilic triterpenoid spacer between the two functional groups.

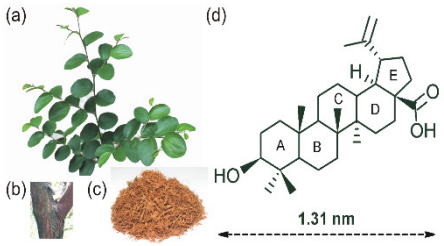

Figure 6. *Ziziphus jujube:* (a) branch (b) stem, (c) bark powder; (d) betulinic acid **2**, a 6-6-6-6-5 pentacyclic monohydroxy triterpenic acid extractable from the bark of *Ziziphus jujube*. The five rings present in the petacyclic triterpene backbone are marked as A, B, C, D, E.

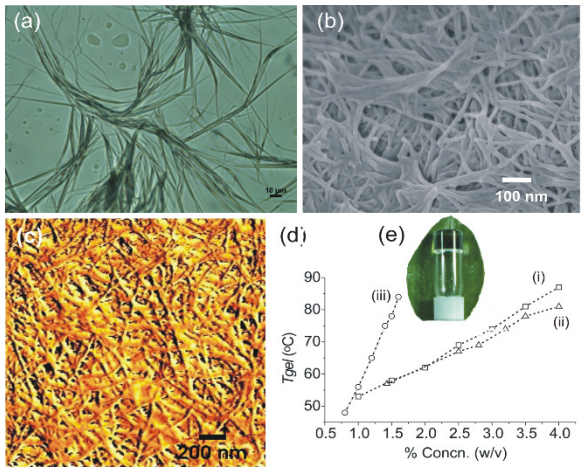

Figure 7. (a) Optical microscopy image of betulinic acid gel in o-dichlorobenzene (0.41 % w/v) showing fibrillar network.; (b) FESEM image of betulinic acid xero-gels in mesitylene (2.04% w/v), (c) AFM images of betulinic acid in p-xylene (c = 1.25% w/v (d) Plot of Tgel vs concentration; (e) inverted vial containing a transparent o-dichlorobenzene gel with *Ziziphus jujube* leaf as the background. Adapted with permission from ref. 53 Copyright 2011 Royal Society of Chemistry.

Even though the molecule was well known to the scientific community for its anticancer, antitumor, anti-HIV and antidiabetic activities,[49,50,51,52] there was no report in the literature on its self-assembly properties. We extracted the compound from the bark of *Ziziphus jujube* as a white solid following an optimized procedure developed our laboratory. In 2011, we reported the spontaneous self-assembly property of betulinic acid in different organic liquids without any derivatization.[53] Among the 22 organic liquids tested, the molecule self-assembled in all liquids yielding strong gels in 19 liquids and remained as a colloidal suspension in 3 liquids (Table 1).

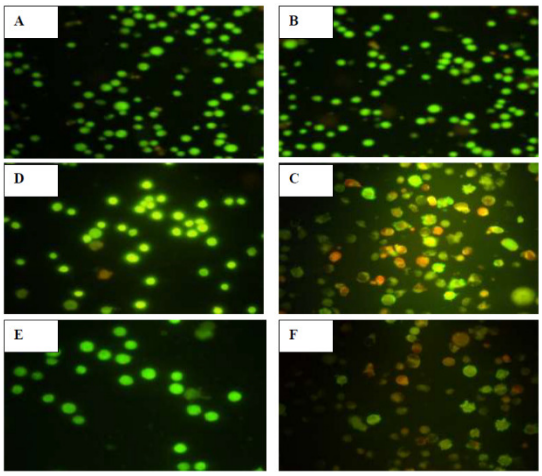

Figure 8. Qualitative characterization of nuclear morphology by fluorescence microscopy at the excitation/emission wave lengths 490/620 nm after dual staining with EtBr/AO: (A): PBL control, (B): PBL treated with BA; (C) KG-1A control, (D): BA treated KG-1A cells, (E): K562 control and (F): BA treated K562 cells.

All the 11 aromatic liquids tested formed strong gels and o-dichlorobenzene, bromobenzene and nitrobenzene could be gelled even at a concentration of less than 1% (w/v).

Strong gels were also obtained in higher homologous alcohols from C3 to C8. Though chloroform did not form a gel among the aliphatic chloro solvents tested, carbon tetrachloride and tetrachloroethane could be gelled efficiently by betulinic acid with carbon tetrachloride turning out to be the best solvent for gelation with minimum gelator concentration of 0.48% (w/v).

Detailed investigation of the morphology of self-assembled betulinic acid in different liquids was carried out by optical microscopy in their native state and by SEM and AFM in xerogel state (Figure. 7). Optical microscopy in the native state revealed micro sized fibrillar network consisting of fibers with 1-4 micrometer cross-sections. Densely packed fibrillar network having fibers of nanometer cross sections and micrometer lengths were observed in the xero-gel samples

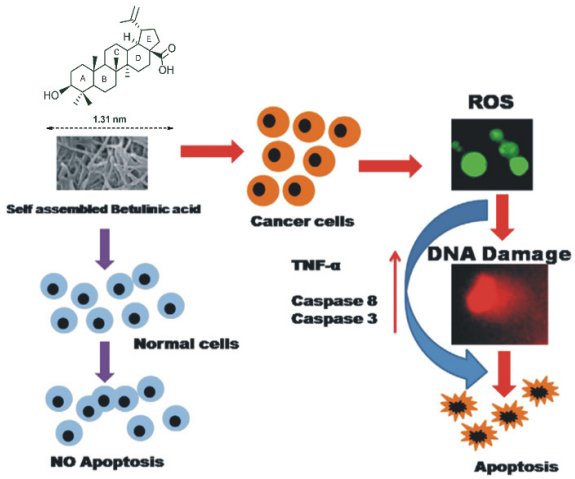

Figure 9: Self-assembled betulinic acid mediated selective leukemic cell death through activation of ROS/TNF-a

from different organic liquids in both SEM and AFM analyses. (Figure. 7). As the molecule was 1.31 nm long, the dimensions of the fibers indicated that several betulinic acid were present both in the lengths and breadths of the fibers. All these analysis indicated that the molecule self-assembled in organic liquids very efficiently in a 1D manner yielding fibers which then formed an entangled 3D fibrillar network. The mobility of the solvent molecules were lost due to entrapment inside network yielding in a supramolecular gel.

Selective damage of cancer cells without affecting the normal cells has been a challenge to the scientific community for Figurehting against the deadly disease.[54] Betulinic acid conjugated with folic acid was found to be selective anticancer agent when studied on KG-1A and K562 cancer cells.[55] Selective anti-leukemic efficacy study of self-assembled betulinic acid (SA-BA) was investigated by cell viability assay. Probable pathway of apoptosis and mode of leukemic cell death were monitored by measuring ROS level, pro and anti-inflammatory cytokine status and expression of caspase-8 and caspage-3 by immunocytochemistry.[56] SA-BA was more efficient compared non-assembled BA toward cancer cells with no relevant toxicity to normal blood cells. Reactive oxygen species (ROS) mediated leukemic cell death was facilitated by SA-BA as confirmed by pre-treatment of N-acetyl- L-cysteine. Induction of apoptosis by SA-BA treatment increased pro-inflammatory cytokines, specifically potentiated TNF-a mediated cell death, confirmed by expression of caspase-8 and caspage-3 by immunocytochemistry.[57] This study explored the better anti-leukemic efficacy of SA-BA over BA and this modification will enrich the use of BA in cancer therapy (Figure. 8, 9).

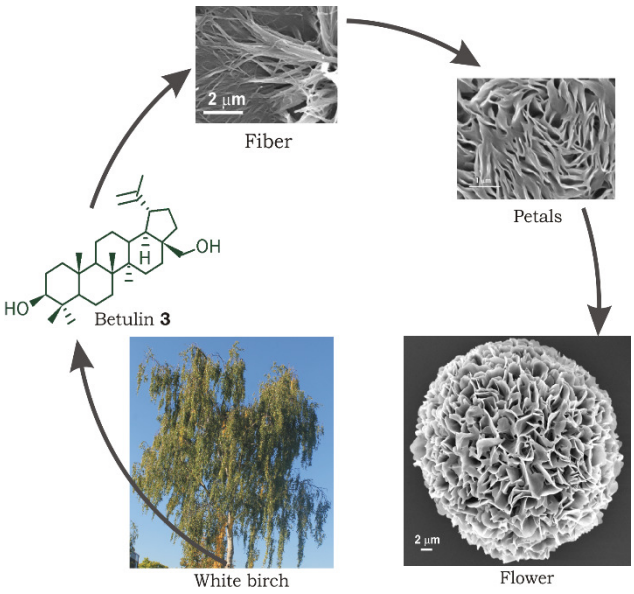

Figure 10. Betulin **3** extracted from bark of White birch spontaneously self-assembles affording flower-like objects consisting of petals and fibers. Reprinted with permission from ref. 60, Copyright 2015 American Chemical Society.

3.3 Self-assembly of betulin 3

The bark of White Birch (*Betula papyrifera*) is rich in betulin **3** (Figure. 10), a 1.29 nm long 6-6-6-6-5 pentacyclic dihydroxy triterpenoid.[58] Anti-tumor, anti-inflammatory and antiviral activities of the compound has been reported.[59] It has a rigid nano-sized lypophilic backbone with uniquely positioned secondary hydroxyl group at the 'A' ring and a hydroxymethyl group at the ring junction of the trans-fused 'D' and 'E' rings. Betulin is identical to betulinic acid **2** except that the 28-COOH group is converted to a hydroxymethyl group at the ring junction of thetrans-fused 'D' and 'E' rings. To gain an understanding about how a minute functional group variation of the triterpenoid molecule can influence it's self-assembly property, we extracted the compound from the bark of white barch and studied the self-assembly property of it molecule in various organic liquids. The dihydroxy triterpenoid self-assembled in aromatic liquids and aqueous solvent mixtures yielding soft solid-like materials in some of the liquids.[60] For instance, an opaque gel was formed instantly in DMSO-water (1:1) at 1% w/v. Whereas opaque gels were formed in neat liquids such as *o*-xylene, *m*-xylene, *p*-xylene also yielded opaque gels at 5% w/v, colloidal suspensions were obtained in benzene, toluene, mesitylene and *o*-dichlorobenzene. Colloidal suspensions were also obtained in mixed solvents like EtOH-water (1:1), DMF-water (1:1) and EG-water (1:1).

Study of the morphology of the self-assemblies of betulin carried out in native state by optical microscopy revealed flower-like morphology of micrometer diameters. Beautiful flower like objects of 5–20 μm were observed by Field Emission Scanning Electron Microscopy (FESEM) in different liquids (Figure. 11). The flowers were composed of dozens of petals (2D sheet) attached to a mutual center and the petals were composed of intertwined fibers of 27–48 nm diameter. The molecule being 1.29 nm long, several molecules are present in the cross-section of the nano fibers. Whereas self-assembled betulinic acid yielded simple fibrillar morphology (as discussed in section 4.1), self-assembled betulin yielded flower like morphology in identical environment. These studies confirmed that minute functional variation, specially the functional group variation at the junction of the trans-fused 'D' and 'E' rings of the triterpenoid molecule, can change the self–assembly properties dramatically. Shifting of the '–O-H' stretching frequencies compared to that in the neat powder in FTIR of different xerogel samples indicated that self-assembly is driven by strong intermolecular H-bonding.

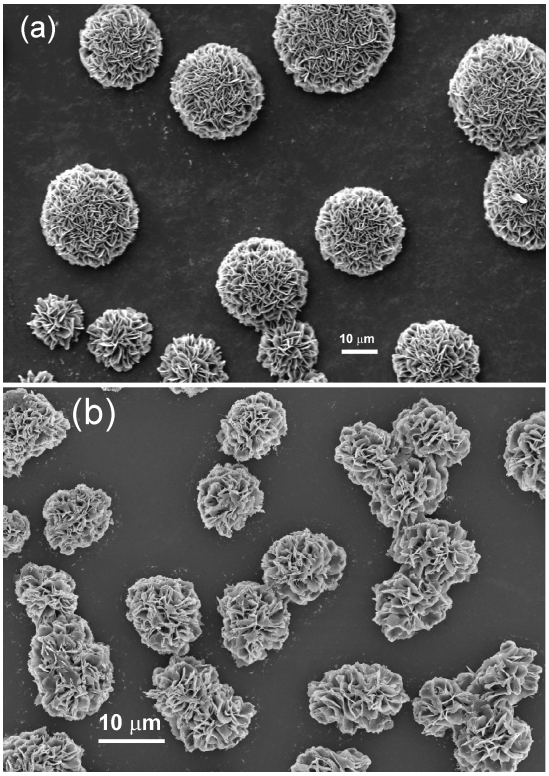

Figure 11. SEM images of dried self-assemblies of betulin prepared from mesitylene liquid (2 % w/v).

To find out whether the porous self-assemblies of betulin are capable of adsorbing various fluorophores, we have studied the adsorption of rhodamine-B and the anticancer drug doxorubicin as model compounds.[61,62,63,64] Microscopic images under normal and fluorescence lights clearly indicated that both the fluorophores were adsorbed on the flower like self-assemblies of betulin (Figure.12a,b). The large surface area of porous self-assembled betulin facilitated the adsorption of rhodamine B and doxorubicin dyes. These results opens up the use of self-assembled betulin in the removal of toxic dyes,[65] and targeted drug delivery vehicles.

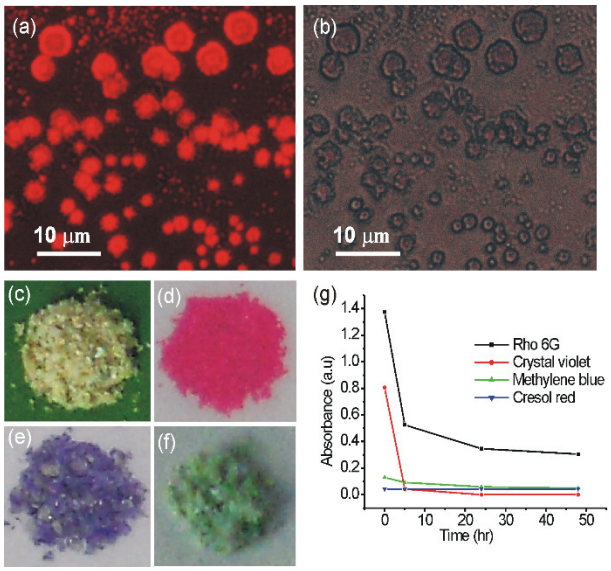

Figure 12. Optical microscopic images of fluorophore adsorbed on self-assembled betulin (1% w/v): (a,b) rhodamine B in isopropanol (0.42 mM), (a) under fluoroscence light. **.** Photograph of dried self-assemblies of **3**: (c) prepared from o-xylene liquid, (d) after adsorption of rho 6G, (e) after adsorption of crystal violet, (f) after adsorption of methylene blue and (g) Plot of absorbance vs time (h) at maximum wavelength (□max) of various dye solutions. . Reprinted (adapted) with permission from ref. 60 Copyright 2015 American Chemical Society.

Whether the dried porous self-assemblies betulin are capable of adsorption of dye molecules, we kept a weighed amount of the dried porous self-assemblies in equilibrium with aqueous solutions of the dyes and the adsorptions of the dyes were monitored by UV–visible spectroscopy after a certain time intervals. The reduction of the absorption intensities with time indicated the adsorption of dye molecules on the surface of the dried porous material. The dried porous self-assembled material could remove the cationic dyes rhodamine 6G (78.0%), crystal violet (99.0%), and methylene blue (62.0%) from aqueous solution very efficiently. Photographs of the porous materials (Figure. 12) after the adsorption of dyes clearly indicated the adsorption of dyes.

Inspired by the spontaneous self-assembly of betulin and betulinic acid in different liquids yielding diversified supramolecular architectures of nano to micrometer dimensions, we became curious to know the self-assembly properties of other triterpenoid molecules.[53] The variations in the triterpenoid framework and the spatial dispositions of the functional groups may have profound effect on the self-assembly property of a triterpenoid molecule. Hence, it occurred to us that oleanolic acid will be a suitable molecule for such investigations.[66] Oleanolic acid 4, a nano-sized 6-6-6-6-6 pentacyclic triterpenoid (Figure.13d), is present in root bark of *Lantana camara* as the free acid.[67] It has tremendous medicinal importance including anticancer and antitumor activities.[68]

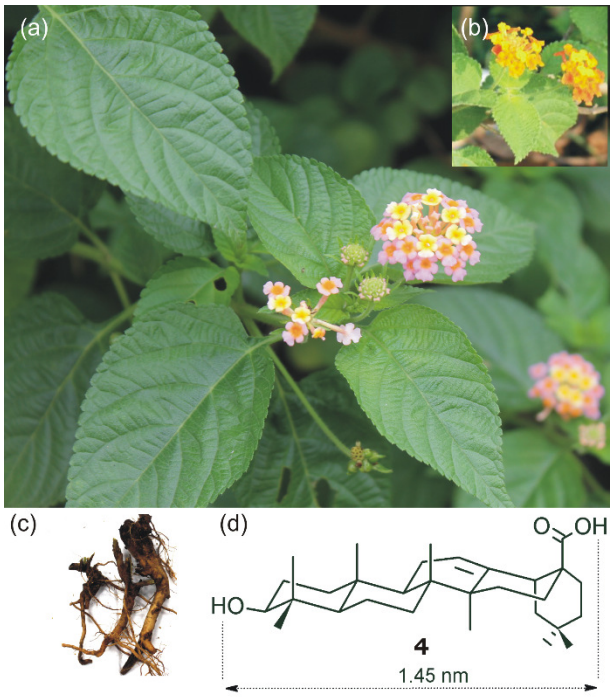

Figure 13. (a, b) *Lantana camara*, (c) root of *Lantana camara*, (d) oleanolic acid

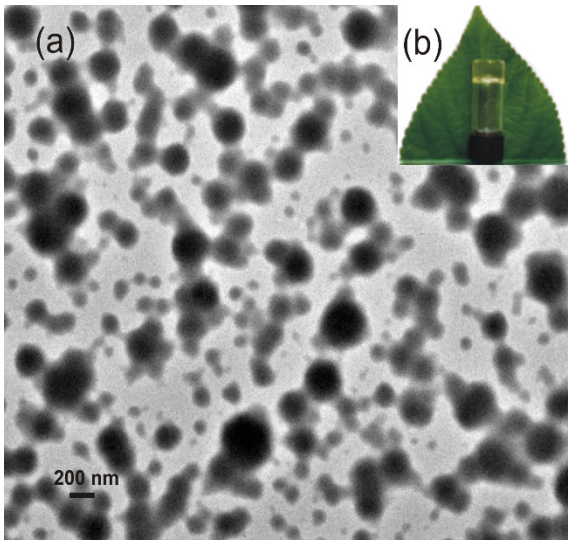

Figure 14. (a) TEM images (unstained) of soft vesicles from a solution of oleanolic acid in chlorobenzene (c = 0.28% w/v) having 99.8 nm ± 9 nm, (b) a gel of **4** in mesitylene with *Lantana camara* leaf at the background. Reprinted (adapted) with permission from ref. 66 Copyright 2012 John Wiley and Sons.

We extracted the oleanolic acid from the root bark of *Lantana camara* following an optimized procedure developed in our laboratory. Self-assembly properties of oleanolic acid were investigated in 25 neat organic liquids, DMSO-water and alcohol-water mixtures.[66] Interestingly, compound **4** showed excellent self-assembly properties in most of the liquids tested and yielded strong gels in 19 liquids including alcohols, aromatic liquids, chloro-alkanes and aqueous binary solvent mixtures. Excellent gels were formed in all the 11 aromatic liquids tested. Homologues alcohols from C3-C5 and C7 and ethylene glycol could be gelled easily and ethylene glycol turned out to be the best solvent for gelation with an MGC of 0.73% (w/v). The observation that a strong gel was obtained in n-butanol but in t-butanol it remained in solution indicated

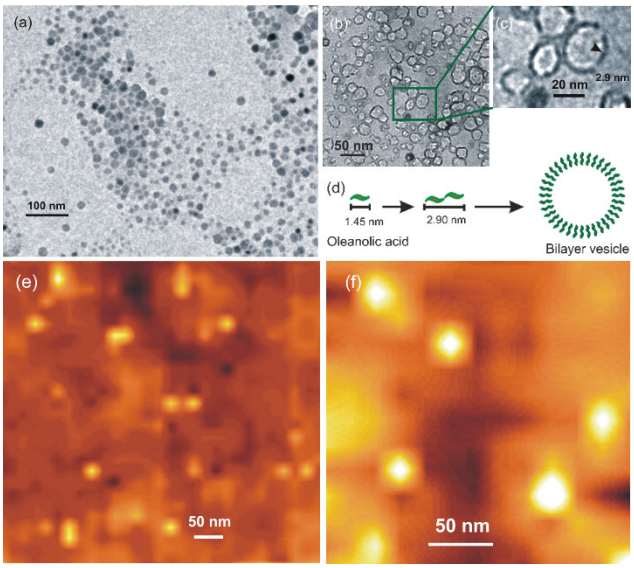

Figure 15. (a-c) TEM images (unstained) of soft vesicles from a solution of oleanolic acid in chlorobenzene (c = 0.11% w/v) having 14 - 23 nm diameter, (d) model proposed for the bilayer vesicle formation from oleanolic acid, (e,f) AFM images of oleanolic acid in chlorobenzene (c = 0.28% w/v); spherical objects of 25-40 nm diameter . Reprinted (adapted) with permission from ref. 66 Copyright 2012 John Wiley and Sons.

the structural sensitivity for gelation. Among the aliphatic chloro solvents tested, compound **4** gelled chloroform and tetrachloroethane easily but remained insoluble in carbon tetrachloride indicating the structural sensitivity of the liquids towards self assembly of the triterpenoids. [53] When compared with betulinic acid **2**, it is important to note that carbon tetrachloride could be gelled easily by betulinic acid **2** but remained insoluble in the analogues oleanolic acid **4**. Structural sensitivity of the analogues triterpenoid molecules towards self-assembly in the same solvent is demonstrated by this observation.

Morphological characterization of the self-assemblies of oleanolic acid was carried out by optical microscopy in their native state and by SEM, TEM and AFM in dry condition. Mostly vesicular self-assemblies were observed in all the studies (Figure. 14, 15). For example, the dried self-assemblies of oleanolic acid **4** in chlorobenzene (0.28%) by transmission electron microscopy revealed spherical self-assembly of average diameter 99.8 nm ± 9 nm (calculated from the diameters of 270 spherical objects) (Figure. 14).[69] As the molecular length of oleanolic acid is 1.45 nm, the membrane thickness of 2.8 - 3.0 nm of the spherical objects indicated that the spherical objects were actually bilayer vesicles (Figure. 15b). The sharp peaks observed by x-ray diffraction studies of the gels of **4** in chlorobenzene and ethylene glycol corresponding to d spacings of 2.90 nm and 2.85 nm respectively also supported a bilayer vesicular structure as observed by TEM studies also supported the bilayer membrane. Intermolecular H-bonding between hydroxyl and carboxyl groups in addition to the dispersive interaction by the non-polar triterpenoid backbone are believed to be the major driving force for the self-assembly.[66]

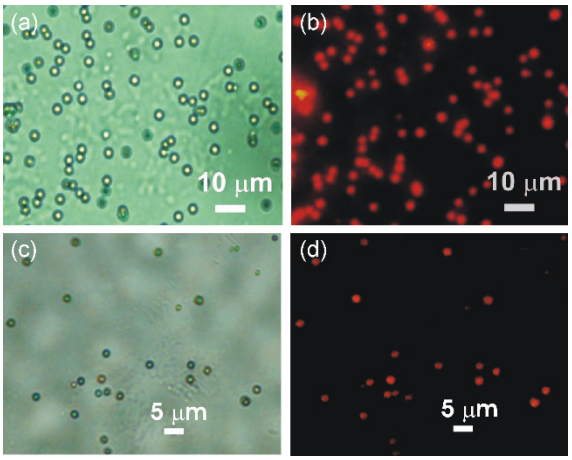

Figure 16. Epifluorescent microscopy images of a solution of oleanolic acid in isopropanol (a-b): c = 31.31 mM containing 0.314 mM rhodamine-B; (c-d): c = 9.96 mM containing doxorubicin (c = 0.33 mM); (a,c) bright field images, , (b,d) fluorescent images. . Reprinted (adapted) with permission from ref. 66 Copyright 2012 John Wiley and Sons.

Vesicular self-assemblies of **4** of 2.5-5.0 μm in aqueous DMSO were observed by optical microscopy media in native state. Aqueous DMSO being a biocompatible medium, we tested the entrapment of fluorophores including the entrapment of the anticancer drug doxorubicin. Interestingly, the cationic dye rhodamine-B and the chemotherapeutic drug doxorubicin were entrapped inside the vesicular self-assemblies as indicated by epifluoroscence microscopy studies (Figure. 16). Entrapment of the anticancer drug doxorubicin inside the vesicular self-assemblies of **4** in a biocompatible medium paves the way for its usefulness as a drug delivery vehicle.[70, 71, 72,73]

3.5 Self-assembly of ursolic acid 5

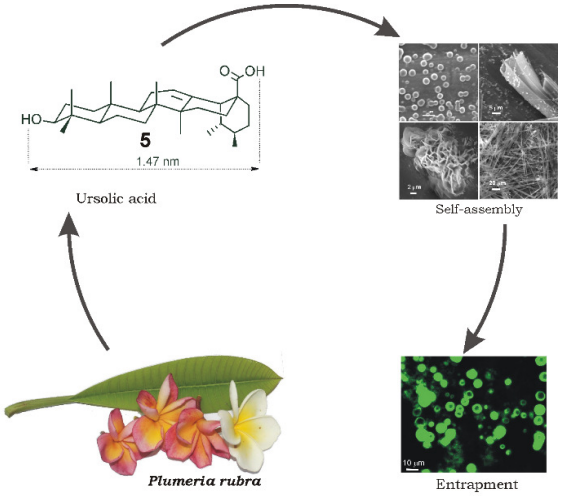

Figure 17. Schematic representation of self-assembly of ursolic acid extractable from *Plumeria rubra* yielding nano-architectures and its use in drug entrapment. Reprinted (adapted) with permission from ref. 83 Copyright 2017 Royal Society of Chemistry.

Ursolic acid, a naturally occurring 6-6-6-6-6 monohydroxy triterpenic acid, is extractable from the leaves of *Plumeria rubra* as a free acid having wide varieties of pharmacological activities. [74,75,76,77,78] Anticancer and antitumor activities of ursolic acid have been reported in different cell lines.[79,80,81,82] Ursolic acid **5**, a ursane type triterpenic acid extractable from the leaves of *Plumeria rubra* will be an interesting molecule for the study of its self-assembly properties in different liquids (Figure. 17). Herein we report that ursolic acid self assembles in different neat liquids as well as aqueous liquid mixtures yielding supramolecular architectures such vesicles, tubes, fibers and flowers of nano- to micro-meter dimensions.[83] The vesicular self-assemblies are capable of entrapping fluorophores including the anticancer drug doxorubicin. Release studies of the entrapped fluorophores including the anticancer drug doxorubicin has also been demonstrated making it useful as a drug delivery vehicle.

Self-assembly of compound **5** was tested in 22 organic liquids and aqueous liquid mixtures. Among the 22 neat organic liquids tested for the self-assembly studies, ursolic acid self-assembled in most of the liquids in the concentration range of 1-6% w/v forming gels in 12 neat liquids. Among the three aqueous liquid mixtures tested for the self-assembly studies, ursolic acid self-assembled in all the aqueous liquids forming a strong gel in DMSO-water. Atomic force microscopy of the dried self-assemblies of **5** prepared from a solution of **5** in ethanol-water (3:1, 0.12% w/v) indicated the formation of spherical self-assemblies of 120 - 360 nm diameters and heights 23-27 nm (calculated from the diameters of 149 spheres). The 3D images clearly indicated the spherical nature of the self-assemblies. The measured heights do not match with radius of the spherical objects due to deformation by the AFM tip indicating a soft nature of the spherical self-assemblies. SEM studies with the dried self-assemblies of **5** prepared from a colloidal suspension in ethanol-water (3:1, 0.23% w/v) indicated poly-disperse spherical self-assemblies of nano- to micrometer diameters (average size of 480 nm calculated from 87 spherical self-assemblies, Figure. 18a).

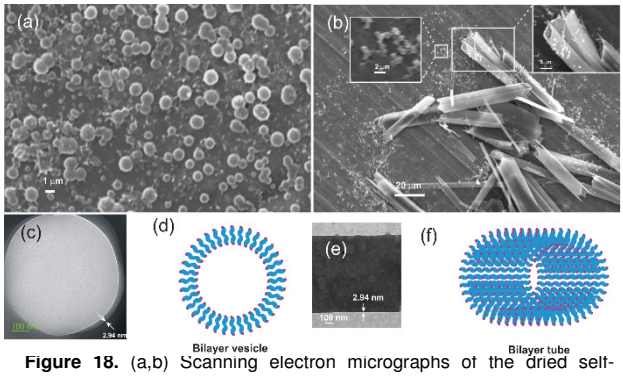

Figure 18. (a,b) Scanning electron micrographs of the dried self-assemblies of ursolic acid prepared from colloidal suspension in ethanol-water (3:1): (a,b) 0.23% w/v, (c) HRTEM (unstained) of self-assembled ursolic acid in mesitylene (0.21% w/v), (d) model bilayer vesicle, (e) tube in ethanol-water (3:1), (f) model tube. . Reprinted (adapted) with

Tubular self-assemblies along with spherical self-assemblies were observed in SEM images of the dried self-assemblies of **5** prepared from a solution in ethanol-water at 0.23% w/v along with certain percentage of fibrillar network (Figure. 18b). HRTEM images of the spherical self-assemblies clearly indicated the vesicular nature of spherical self-assemblies (Figure. 18c). With the membrane thickness of 2.94 nm and the molecular length being 1.47 nm, a bilayer vesicular structure is proposed (Figure. 18d). The membrane thickness of the nano-tubes observed by HRTEM was also 2.94 nm (Figure. 18e) supporting bilayer morphology of the tubular self-assemblies (Figure. 18f). The bilayer membrane morphology is supported by X-ray diffraction studies of a gel of **5** in m-xylene (2.1% w/v) that revealed a sharp peak at 2Θ=3.0, which corresponds to a d spacing of 2.94 nm .

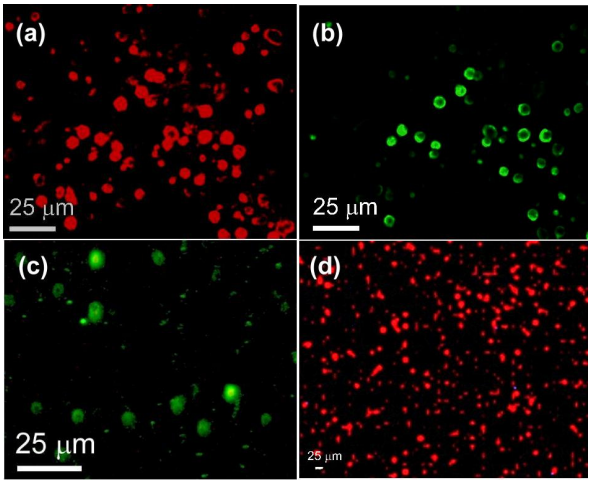

Figure 19. Epifluorescent microscopy images of self-assembled ursolic acid (a-c) in ethanol-water (3:1, 30.13 mM): (a) containing Rodamine-B (0.30 mM) exposed under green emission light, (b) containing Rodamine-B (0.30 mM) exposed under blue emission light, (c) containing CF (0.30 mM) exposed under blue emission light, (d) in ethanol-water (3:1, 22.93 mM) containing doxorubicin (2.2 mM) exposed under green emission light.Reprinted (adapted) with permission from ref. 83Copyright 2017 Royal Society of Chemistry.

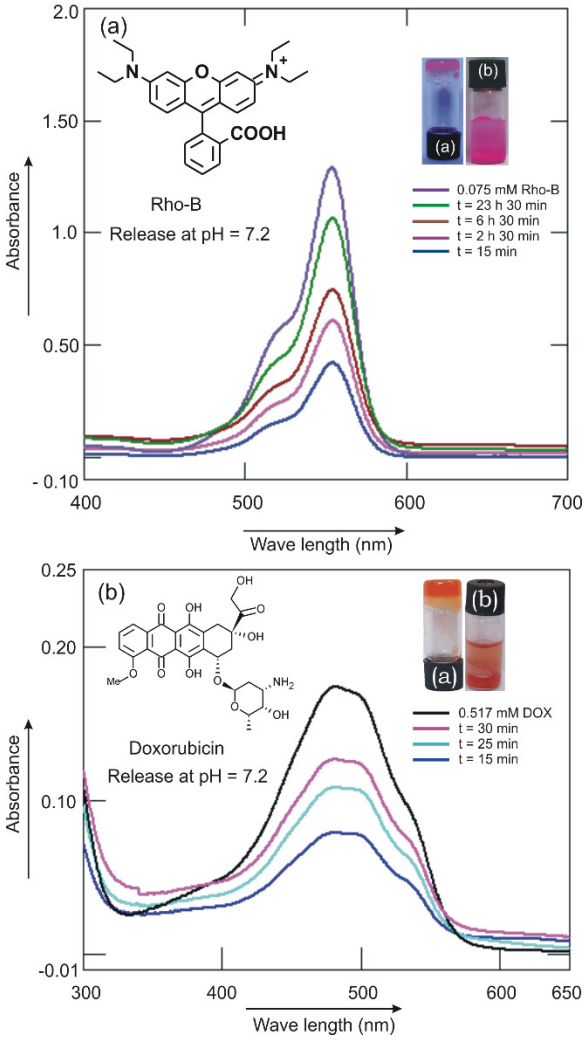

Figure 20. (a) Release of the ursolic acid (55 mM) gel-entrapped fluorophore Rho-B (0.54 mM): overlay of the UV-visible spectra of the released Rho-B to buffers at pH 7.2 at various time intervals, (b) release of the ursolic acid (56.1 mM) gel-entrapped anticancer drug doxorubicin (0.51 mM) in buffer solution at (a) pH = 7.2: overlay of the UV-visible spectra of the released doxorubicin to buffers at various time intervals. . Reprinted (adapted) with permission from ref. 83 Copyright 2017 Royal Society of Chemistry

Development of biocompatible nano carriers has been an emerging area of research for efficient and targeted drug delivery with an aim to minimize the serious side-effects in chemotherapy.[84,85,86,87] Whether the vesicular self-assemblies of **5** are capable of entrapping drug molecules, we initially examined the entrapment of the cationic dye Rhodamine B (Rho-B) and the anionic dye 5,6-carboxyfluorescein (CF). To our delight, we observed that the vesicular self-assemblies were capable of entrapping both the fluorophores (Figure.19a,b and c). Inspired by these results, we examined the entrapment of anticancer drug doxorubicin. Reddish fluorescence observed from the vesicular self-assemblies indicated entrapment of the chemotherapeutic drug (Figure. 19 d).

Release study of the entrapped dye molecules to buffer solutions at physiological pH (7.2) is an integral part of the drug entrapment studies for prospective use of the self assemblies in drug delivery experiments.[88,89,90,91] To examine this, initially a Rho-B (0.54 mM) loaded gel of ursolic acid (54.8 mM) in DMSO-water (5:3, 0.16 mL) was covered with a buffer solution (10 mM, 1 mL, pH 7.2) and the release was monitored by UV-visible spectroscopy at various time intervals. A significant release of the Rho-B (87%) was observed after 23 h 30 min (Figure. 20a). Inspired by this observation, release study of the anticancer drug doxorubicin was carried out from doxorubicin-laded gel at physiological pH (7.2) and low pH (6.6) environment of hypoxic tumor or endosomes. A significant release of the anticancer drug doxorubicin at physiological pH (7.2) after 30 min 75% of the drug was released and at the low pH environment 88% released after 60 min, making it useful for prospective drug delivery (Figure 20b).

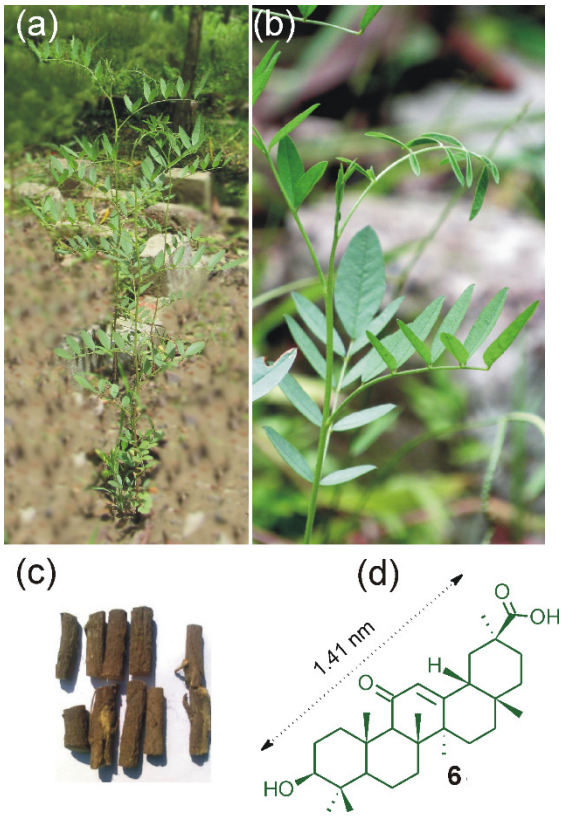

Figure 21. (a,b). Schematic representation of self-assembly of *18β-glycyrrhetinic acid* **6** affording spherical and flower-like objects yielding a gel. (b) A gel of **6** in bromobenzene with crushed *Glycyrrhiza glabra* root at the background.

3.6 Self-assembly of glycyrrhetinic acid 6

18β-glycyrrhetinic acid **6** is extractable from the root of *Glycyrrhiza glabra* (Figure. 21). The root *Glycyrrhiza glabra* is widely used as a traditional medicine for treatment of throat problem. On oral consumption, the sweetening agent glycyrrhizin present in the root is converted to 18□-glycyrrhetinic acid in the human intestine.[92] Application of 18□-glycyrrhetinic acid has been demonstrated as an

antiinflammatory, anticancer and antitumor drug and a nutraceutical for remedying lung diseases and its in-vivo assays have also been carried out.[93,94] Success in the self-asssembly of pentacyclic triterpenoids **2**-**5**, encouraged us to study the self-assembly of 18□-glycyrrhetinic acid **6** in different liquids. It is a 1.41 nm long 6-6-6-6-6 pentacyclic mono hydroxyl triterpenic acid with an enone moiety in the 'C' ring. The structural difference with the previously studied 6-6-6-6-6 triterpenic acid **4** and **5** is the attachment of the carboxyl group at the 'E'-ring and not at the junction of the cis fused 'D' and 'E' rings. The hydroxyl and the carboxyl groups are 1.09 nm apart and separated by the rigid 6-6-6-6-6 pentacyclic backbone spacer. We isolated the compound **6** from the root of *Glycyrrhiza glabra* by following an improved method developed in our laboratory and studied its self-assembly properties in different liquids.[95]

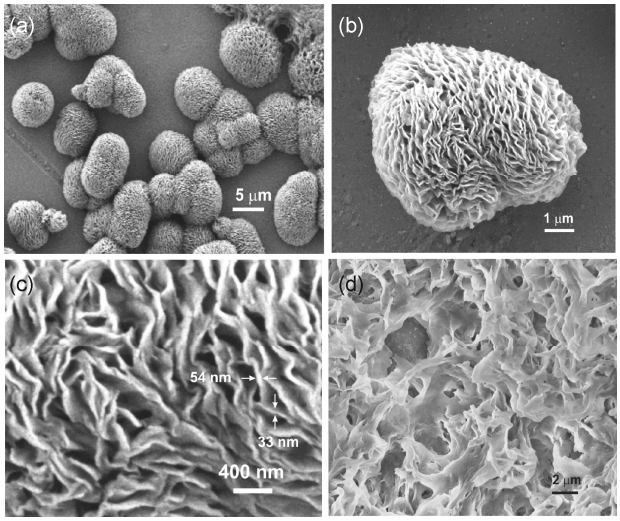

Figure 22. FESEM image of 18β -glycyrrhetinic acid xerogel in (a-c) nitrobenzene (0.25% w/v) (d) o-dichlorobenzene (0.25% w/v) Reprinted (adapted) with permission from ref. 95 Copyright 2012 Royal Society of Chemistry.

Among the 22 liquids tested for self-assembly, the triterpenoid **6** self-assembled in most of the liquids yielding strong gels in 15 liquids and colloidal suspensions in the 4 liquids. Morphology of the self-assemblies studied optical microscopy and AFM revealed spherical self-assemblies. Thorough analysis by FESEM revealed flower like self-assemblies composed of 2D-sheets of 33–88 nm thickness. The 2D sheets were composed of intertwined fibers of 30–40 nm cross-sections (Figure. 22 and 23). As the triterpenoid **6** is 1.41 nm long, the dimensions of the fibers indicate that several 18□-glycyrrhetinic acid molecules must be present in the length and the bredth of the fibers.

The major driving force for the self-assembly of the molecules is believed to be H-bonding involving the carboxyl and hydroxyl groups in addition to the dispersive interactions by the triterpenoid backbones. Evidence for the involvement of H-bonding by the carboxyl groups was obtained by FTIR studies where a shift of the 'C=O' stretching frequency was observed from 1705 cm^{-1} in a powder sample to 1695 cm^{-1} in the gel sample in o-dichlorobenzene. The stretching frequencies of the 'C=O' group in the xerogels prepared from chlorobenzene, bromobenzene, nitrobenzene, o-dichlorobenzene appeared at 1702, 1702, 1702, 1703 cm^{-1} respectively indicating a shift of 2–3 cm^{-1} compared to that in the powder. The identical 'C=O' stretching frequency values observed in the xerogels indicated that the 'C=O' groups were in identical H-bonded environments.[96]

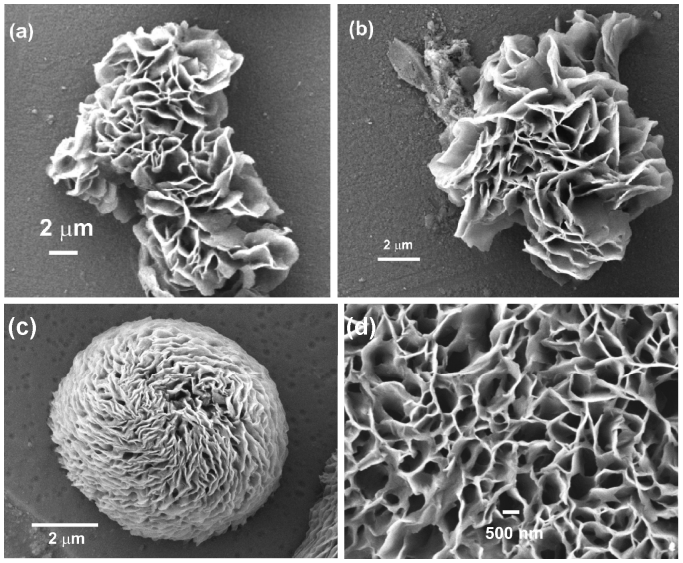

Figure 23. FESEM image of 18β-glycyrrhetinic acid **6** xerogel at 0.25% (w/v) concentration in: (a,b,d) nitrobenzene (0.25% w/v) (c) o-dichlorobenzene (0.25% w/v), Reprinted (adapted) with permission from ref. 95 Copyright 2012 Royal Society of Chemistry.

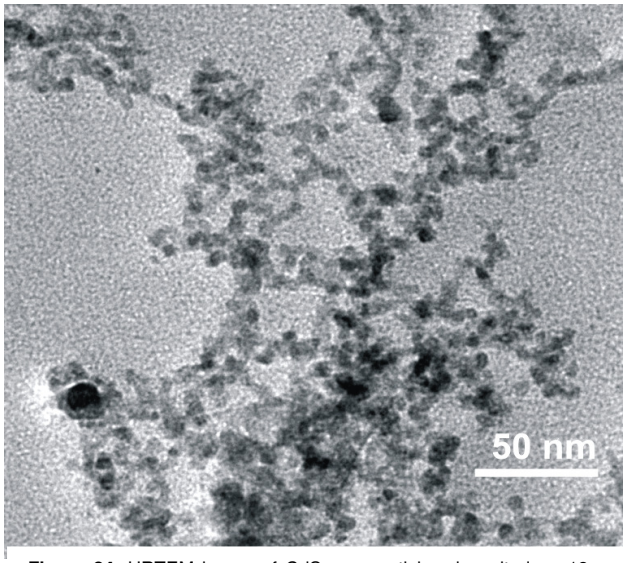

Figure 24. HRTEM image of CdS nanoparticles deposited on 18□-glycyrrhetinic acid self-assemblie. Reprinted (adapted) with permission from ref. 95 Copyright 2012 Royal Society of Chemistry.

Templated growth of CdS nanoparticles (CdSNP) in the form of nano and micro sized spherical objects and fibers has become an area of intense research because of their applications in industry as well as advanced areas such as biological labelling, light emitting diodes, photoelectronic

devices, etc.[97,98,99] As the 3D flower-like self-assemblies of 18□-glycyrrhetinic acid **6** have very high surface area, we utilized those self-assemblies for the templated growth of CdSNPs.[95] When a solution of 18□-glycyrrhetinic acid **6** in ethylene glycol (0.2 mL, 1 % w/v) and cadmium acetate (5 mM) were kept under H_2S atmosphere for 30 s instant appearance of light yellow color in the reaction mixture indicated the formation of CdSNPs. HRTEM studies, energy dispersive X-ray spectroscopy (EDX) and X-ray diffraction confirmed the formation of CdSNPs on the self-assembled microstructures (Figure 24).

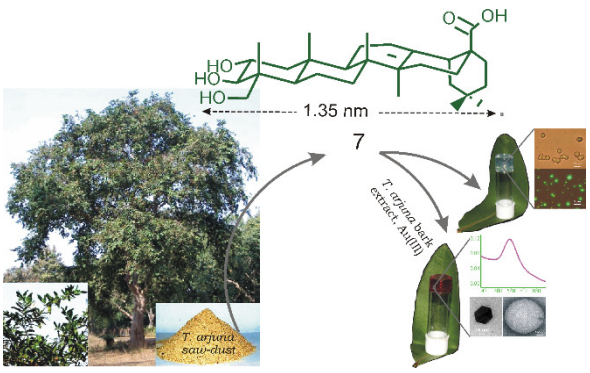

Figure 25. Schematic representation of the formation of gel and gel–gold nanoparticle hybrid material from arjunolic acid 7 extractable from the saw-dust of Terminalia arjuna (inverted vials containing gels with the leaves of Terminalia arjuna in the background: [A] gel of arjunolic acid in ethanol–water (3:4), [B] gel–gold nanoparticle hybrid material. . Reprinted (adapted) with permission from ref. 101 Copyright 2014 Royal Society of Chemistry.

3.7 Self-assembly of arjunolic acid 7

Arjunolic acid **7** (Figure 25), a nano-sized, chiral, 6-6-6-6-6 pentacyclic trihydroxy triterpenic acid is present in the heavy wood of the medicinal plant *Terminalia arjuna* as the free acid. It has a rigid backbone with two equatorial hydroxyl and one equatorial hydroxymethyl groups attached at the 'A' ring. The carboxyl group is situated at the ring junction of the cis fused 'D' and 'E' rings. The compound was extracted from the finely powdered heavy wood of *Terminalia arjuna* and purified by a chemical route, developed in our laboratory, as a white crystalline solid.[100]

Self-assembly properties of arjunolic acid **7** in aqueous medium and study of its utilization as drug delivery vehicle was reported by us in 2014.[101] As anticipated, the molecule with a rigid lypophilic backbone with three hydroxyl and one carboxyl groups at the opposite ends, was poorly soluble in most of the common organic liquids except in polar solvents like DMSO, DMF, acetonitrile, etc. Interestingly, in aqueous binary solvent mixtures such aqueous ethanol, DMSO, DMF or ethylene glycol, arjunolic acid showed a tendency to self-assemble yielding spherical self-assemblies and gels at certain concentrations of arjunolic acid and solvent compositions (Table 2). The positive free energy change (ΔG°) during gel to sol transition calculated from T_{gel} vs. concentration plots indicated the stability of the gels[101]

Table 2. Gelation test results of arjunolic acid **7** in aqueous solvents

Serial No.[a]	Medium (v/v)	State	MGC	*Tgel*[b]
1	EtOH/H_2O (3:4)	G	0.11	34
2	DMSO/H_2O (5:4)	G	7.1	67
3	DMF/H_2O (5:3)	G	7.1	35
4	EG/H_2O (3:1)	VS	2.5	..

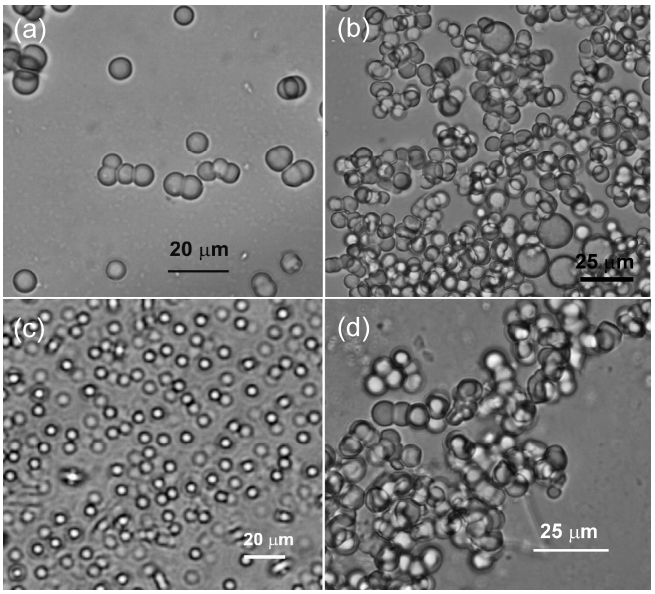

Figure 26. Optical microscopy images of self–assembled arjunolic acid in (a,b) DMSO-water (5:4) at (a) 5.55% w/v, (b) 7.1% w/v; (c,d) DMF-water (5:2) at (c) 0.10 % w/ v (d) at 6.25 % w/v. Reprinted (adapted) with permission from ref. 101 Copyright 2012 Royal Society of Chemistry.

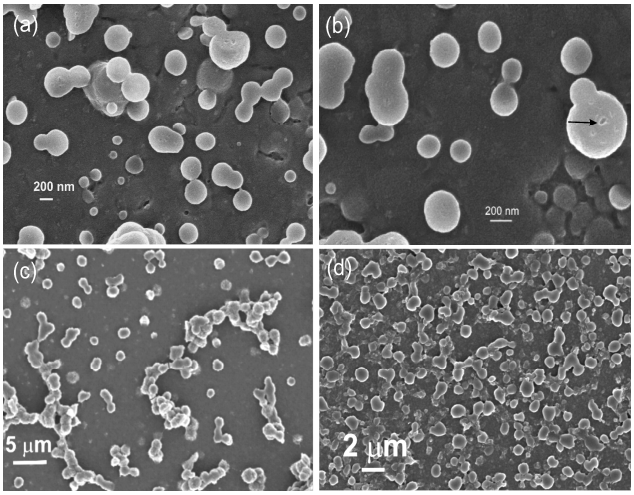

Figure 27. FESEM of dried self-assemblies of arjunolic acid in (a,b) ethanol-water (3:4, 0.11 % w/v) at MGC, (c) DMF-water (5:2, 0.71 % w/v); (d) DMSO -water (5:2, 0.71 % w/v). Reprinted (adapted) with permission from ref. 101 Copyright 2014 Royal Society of Chemistry.

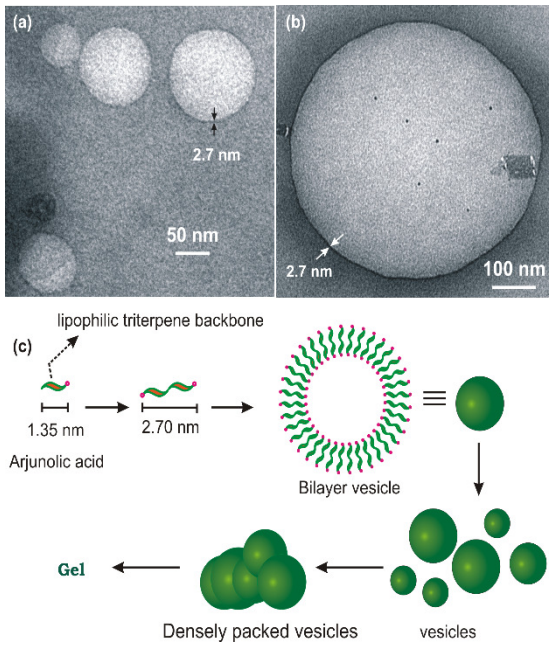

Figure 28. TEM images of self-assembled arjunolic acid in (a) DMSO–water (1:1, 0.022% w/v); (b) ethanol–water (3:4 ratio, 0.043% w/v) with gold nanoparticles. (c) Schematic representation of the formation of supramolecular gel via formation of bilayer vesicles. . Reprinted (adapted) with permission from ref. 101 Copyright 2014 Royal Society of Chemistry.

Discrete spherical self-assemblies at a lower concentration and densely packed spherical self-assemblies at a higher concentration of arjunolic acid were observed by both optical microscopy (Figure 26) in native state and FESEM for the xero-gels (Figure 27). FESEM studies carried out with the dried Self-assemblies of arjunolic acid (0.11% w/v) at its MGC from aqueous ethanol (3:4) indicated the formation of nano-sized spherical objects with an average diameter of 185 nm. Sharp contrast between the centre and the distinct periphery observed in the dried spherical self-assemblies of arjunolic acid by HRTEM analysis indicated that the spherical self-assemblies were actually vesicular in nature (Figure 28). The molecular length of arjunolic acid being1.35 nm and the measured membrane thickness of the vesicles by HRTEM analysis being 2.7 nm, a bilayer vesicular membrane is proposed (Figure. 28). The low angle X-ray diffraction studies carried out with a gel sample of arjunolic acid in DMF–water (7.1% w/v, 5:2 v/v) revealed a peak at 3.82° corresponding to a d-spacing of 2.68 nm, also supported a bilayer membrane structure of the vesicles (Figure. 28 b). Based on these observations, a mechanism for the formation of gel via vesicular self-assemblies is proposed (Figure. 28 c). The reports of vesicular gel specially the vesicular self-assembly of naturally occurring low molecular mass organic compounds are not common in the literature compared to fibrillar gels.[102] The major driving force for the self-assembly was intermolecular H-bonding between the hydroxyl and carboxyl groups in addition to the dispersion interaction by the triterpenoid backbone. Evidence for the involvement of H-bonding came from the FTIR studies, where shifting of both the 'C=O' and 'O–H' stretching frequencies the powder sample of arjunolic acid to the lower frequency region was observed in all the xero-gel samples indicating.

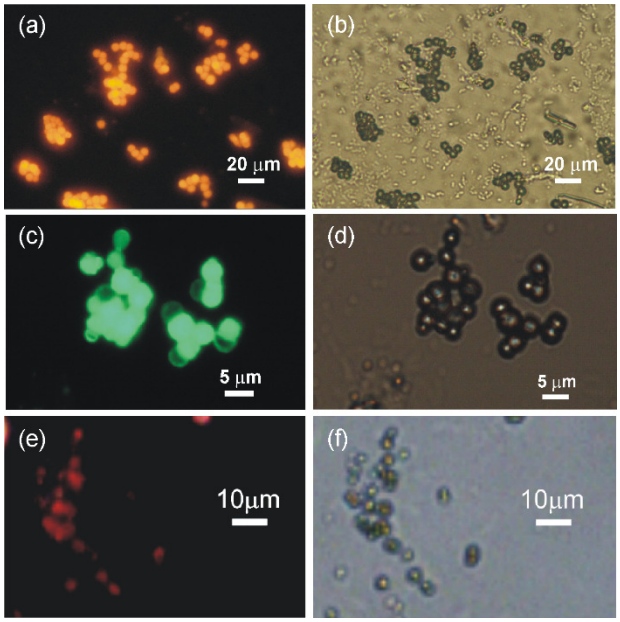

Figure 29. Epifluorescence microscopy images of (a–b) self-assembled arjunolic acid **7** (10.23 X 10-2 M) in DMSO–water (7: 3) containing rhodamine B (5 X10-3 mM), (c–d) self-assembled arjunolic acid (63.9 mM) in DMSO–water (7:3) containing 5(6)-carboxyfluorescein (0.25 mM) (e–f) self-assembled arjunolic acid (1.29 mM) in DMSO–water (5 : 3) containing doxorubicin (4.04 X 10-3 mM); (a, c and e) fluorescent images; and (b, d and f) bright-field images. Reprinted (adapted) with permission from ref. 101 Copyright 2014 Royal Society of Chemistry.

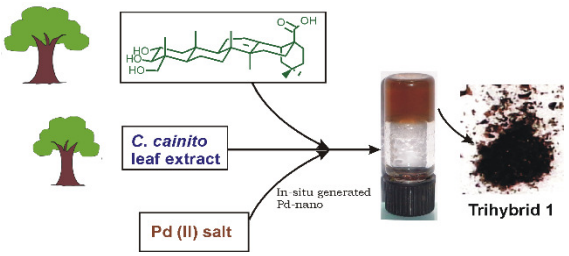

Figure 30: Schematic representation of the geneation of a trihybrid material **1** from the extracts of two plants and its utilization as a recyclable catalyst for organic transformations. Reprinted (adapted) with permission from ref. 105 Copyright 2016 John Wiley and Sons.

There has been an immense research interest in recent years in the utilization of vesicles as drug delivery vehicle.[103] Entrapment studies were carried out with the cationic dye rhodamine B, and the anionic dye CF and the well known anticancer drug doxorubicin and examined by epifluorescence microscopy. Highly intense fluorescence observed from the vesicular self-assemblies under epifluorescence microscopy indicated the entrapment of the fluorophores including the chemotherapeutic drug (Figure 29).To examine the usefulness of self-assembled arjunolic acid as a drug delivery vehicle, controlled release of the entrapped drug molecules to buffer solutions at physiological pH was carried out.[104] A slow and controlled release of the loaded doxorubicin drug from the

arjunolic acid gel in aqueous ethanol medium to the buffer solutions at physiological pH was observed which confirmed its usefulness as a prospective drug delivery vehicle. In another application, a gel-gold nanoparticle hybrid material has been generated under very mild conditions from self-assembled arjunolic acid, the bark extract of *Terminalia arjuna* and Au(III).[101]

4. Generation of arjunolic acid PdNP tri-hybrid and study of its catalytic activities

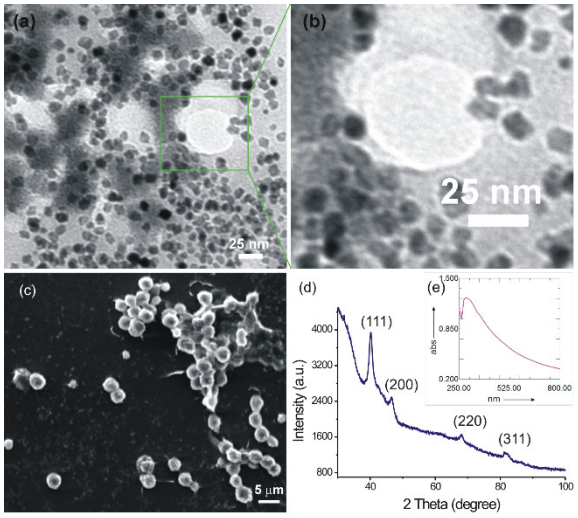

Figure 31. Optical microscopy image of the trihybrid material **1** in native state, (b-c) SEM images of the dried assemblies of trihybrid material 1, (d) XRD of xerogel of trihybrid material 1, (e) SPR band of PdNPs in the trihybrid material **1**. Reprinted (adapted) with permission from ref. 105 Copyright 2016 John Wiley and Sons.

Palladium nanoparticles (PdNPs) have drawn significant attention in recent years because of its usefulness as catalysts for C-C coupling reactions. Recently a few reports have appeared on PdNPs based advanced materials synthesized by utilizing solid organic–inorganic supports such as graphene, zeolites, mesoporous silica, tetraalkyl ammonium salts, ionic liquids, and polymers as stabilizers for their use as heterogeneous catalysts . But the reports of hybrid materials based on renewable and nontoxic precursors are not very common in literature which is very significant for sustainable development.

A novel organic-inorganic trihybrid material has been reported by us recently via in-situ generation of palladium nanoparticles (PdNPs) in a hybrid gel matrix based on renewable chemicals (Figure 30).[105] The constituents of the hybrid gel were a pentacyclic triterpenoid arjunolic acid 7 extractable from *Terminalia arjuna* and the leaf extract of *Chrysophyllum cainito* (LECC) rich in flavonoids. The flavonoid molecules present in the hybrid gel matrix to generated the advanced trihybrid gel via in-situ reduction of doped Pd(II) salts to stable palladium nanoparticles (PdNPs). Detailed morphological characterization of the trihybrid material by various instrumental techniques confirmed the generation of discrete PdNPs of 9 nm size along with the densely packed vesicles in to the trihybrid material 1 (Figure 31).

The xerogel of the trihybrid material was utilized as a recyclable heterogeneous catalyst for two C-C coupling reactions namely Suzuki reaction and Heck reaction and two reduction reactions namely borohydride reductions of 3-nitropenol and 4-nitrophenol. For both the C-C coupling reactions, the catalyst could be recycled upto 4th cycle without significant loss of the catalytic activities.

For the borohydride reduction reactions of 3- and 4-nitrophenols, the trihybrid material 1 acted as a catalyst with 100% yield upto 4th cycle. For example, with 3-nitrophenol as the substrate, the 1st, 2nd, 3rd and 4th cycles completed within 0.5 min, 2 min, 4 min and 7 min respectively with 100% yield which confirming the excellent efficacy of the material as catalyst. Similarly, with 4-nitrophenol as the substrate, the 1st, 2nd, 3rd and 4th cycles completed within 5 min, 13 min, 20 min, and 26 min respectively with 100% yield which again confirming the efficacy of the material as recyclable heterogeneous catalyst for the reduction reactions109.

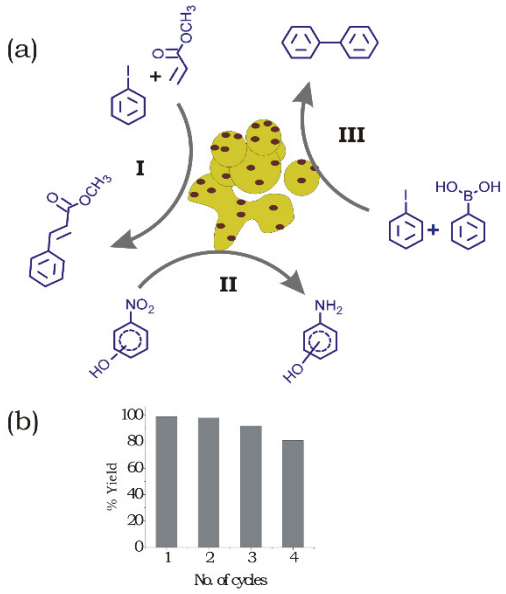

Figure 32: (a) Schematic representation of the utilization of trihybrid material **1** as a recyclable catalyst in Heck and Suzuki reaction and reduction reactions. (b) Plot of % yields vs no. of cycles. Reprinted (adapted) with permission from ref. 105 Copyright 2016 John Wiley and Sons.

3.8 Self-assembly of □-onocerin 8

Inspired by the spontaneous self-assembly of triterpenoids **2**-**7** in different liquids yielding supramolecular architectures such as vesicles, fibers, flowers and tubules of nano to micrometer dimensions, we became curious to study the self-assembly properties of a dihydroxy seco-tetracyclic

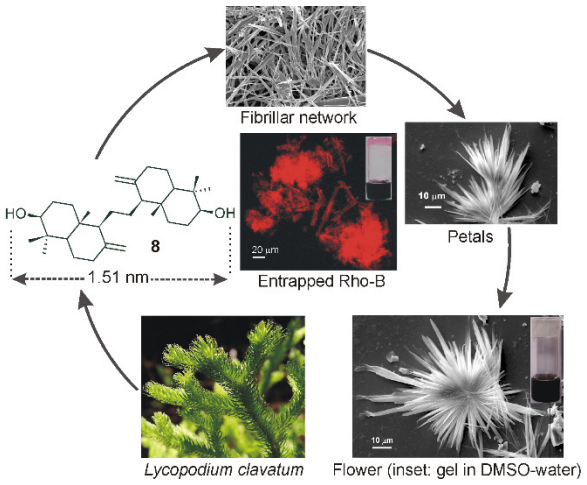

Figure 33. Schematic representation of self-assembly of □-onocerin **8** yielding a gel via fibrillar network and flower-like self-assemblies. Reprinted (adapted) with permission from ref. 107 Copyright 2017 John Wiley and Sons.

triterpenoid α-onocerin **8** [8, 14-seco-gammacera-8, 14-diene-3, 21-diol]. The compound is present in the aerial part of *Lycopodium clavatum*, a spore-bearing vascular plant, growing up to 1 m in height. The molecule has a unique C2-symmetric structure consisting of two independent trans-decalin C_{15} building blocks having two hydroxyl groups at the two ends of the molecule. The molecule **8** was extracted from the aerial part of *Lycopodium clavatum* and purified by an optimized procedure developed in our laboratory, as a white powder[106].

As the molecule contains two hydroxyl groups at the two opposite ends, it is expected to be involved in stabilizing the self-assemblies by intermolecular hydrogen bonding in addition to the dispersive interactions provided by the lypophilic backbone[60]. Indeed self-assemblies were observed in nine of the fifteen organic and aqueous-organic liquids tested, yielding gels in six liquids[107].

The morphology of the self-assemblies of **8** prepared from the colloidal suspensions in o- and m- xylenes (1.1 % w/v), o-dichlorobenzene (2.1% w/v), chlorobenzene (1.0 % w/v), bromobenzene (1.1 % w/v), dodecanol (4.2 % w/v), DMSO (0.1 % w/v and 0.05% w/v) and DMSO-water (0.1% w/v, 1:1 v/v) were examined by scanning electron microscopy. Fibrillar network along with flower-like self-assemblies were observed in most of the dried self-assemblies (Figure. 34). Symmetrical flower-like self-assemblies were observed in o-dichlorobenzene (2.1% w/v) with 0.4-1.64 µm diameter (Figure. 34 a). Flower and petal-like self-assemblies were also observed in the samples prepared from m-xylene (1.5% w/v) and o-xylene (1.1 % w/v) (Figure. 34 b, c). Fibrillar network was observed in DMSO-water (0.1% w/v, 1:1 v/v) and DMSO (0.1 % w/v) with individual fibers having cross sections of 76.8 - 92.2 nm diameters (Figure. 34d) and several micrometer in lengths. To get further insight into the morphologies of the self-assemblies, HRTEM and AFM studies were carried out. Intertwined fibrillar networks having fibers of nano- to micro-meter cross-sections and micrometer lengths were observed in the dried self-assemblies of **8** prepared from the colloidal

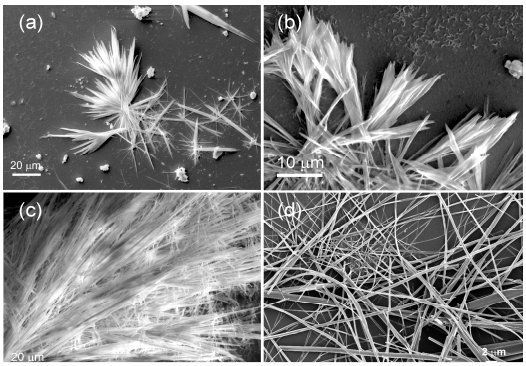

Figure 34. Scanning Electron Microscopic image of **8** in: (a) o-dichlorobenzene (2.1% w/v); (b) m- xylene (1.1 % w/v); (c) o- xylene (1.1 % w/v); (d) (1:1 v/v) DMSO-water (0.1% w/v). Reprinted (adapted) with permission from ref. 107 Copyright 2017 John Wiley and Sons.

suspensions in o-dichlorobenzene (0.21% w/v) by HRTEM studies (Figure. 35 a, b). Intertwined fibrillar network having nanometer cross-section and micrometer length were also observed by AFM in the dried samples prepared from colloidal suspensions of **8** in m-xylene (0.23 % w/v) and o-dichlorobenzene (0.26 % w/v) (Figure. 35 c, d). All these observations support the results obtained by FESEM studies (discussed earlier). Based on these observations a mechanism of the formation of the self-assemblies from the individual components has been proposed as shown in (Figure. 34).

Detailed analysis of the morphologies of the self-assemblies discussed earlier indicated mesoporous morphology of the self-assemblies. Porous morphology with very high surface areas is highly accessible to neutral molecules or ions.[60, 101, 83] To find out whether the self-assemblies of **8** can be utilized for the entrapment and release of fluorophores, we examined the entrapment studies of Rho-B in water (0.020 mL, 0.9 mM) with the self-assemblies in

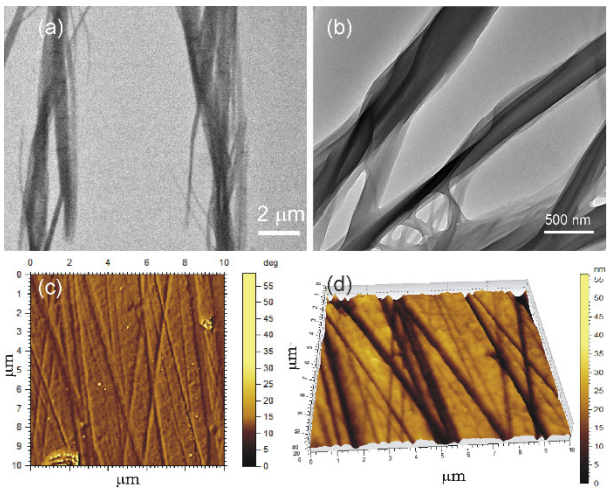

Figure 35. (a,b) HRTEM image of **8** in o-dichlorobenzene (0.21% w/v), (c,d) AFM images of dried self-assemblies **8** in m-xylene (0.23 % w/v); (c) phase diagram, (d) 3D image. Reprinted (adapted) with permission from ref. 107 Copyright 2017 John Wiley and Sons.

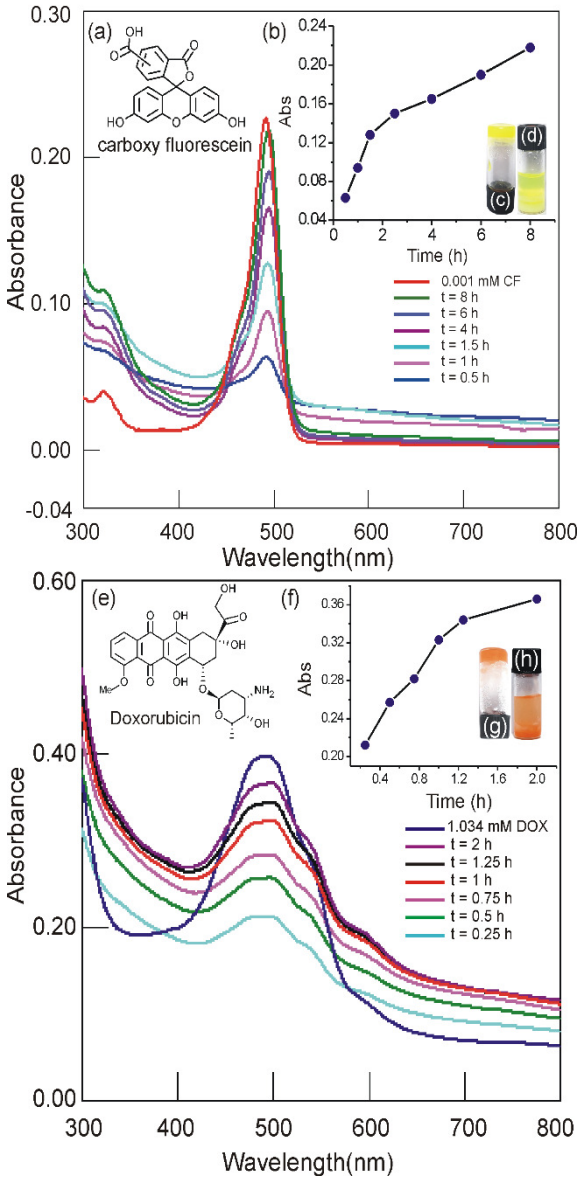

Figure 36. (a) Overlay of UV-visible spectra of released CF into buffers at pH 7.2 at various time intervals from a gel of **8** (36.1 mM) in DMSO-water (1:1 v/v) loaded with CF (0.30 mM); (b) plot of absorbance vs time at 495 nm; (c) photograph of inverted vial containing CF loaded gel; (d) photograph of vial after 8 h of release. (e) Overlay of UV-visible spectra of released doxorubicin, entrapped in a gel of **8** (36.2 mM) in DMSO-water (1:1 v/v) loaded with doxorubicin (5.17 mM) into buffers at pH 7.2 at various time intervals; (f) plot of absorbance vs time at 481 nm; (g) photograph of vial containing doxorubicin loaded gel; (h) photograph of vial after 2 h of release. Reprinted (adapted) with permission from ref. 107 Copyright 2017 John Wiley and Sons.

DMSO-water (1:1, 9.04 mM). Bright red fluorescence from the self-assemblies when observed by epifluorescence microscopy indicated the entrapment of the fluorophores in the self-assemblies (Figure 30).

Successful release of the entrapped drug molecules into the target site is an integral part of an effective drug delivery system. To examine whether the entrapped fluorophores on the self-assemblies of **8** can be released, we carried out the release studies of Rho-B and CF into PBS buffer (pH 7.2).

When a Rho-B (0.47 mM) loaded gel of **8** (28.25 mM, 0.25 mL) in DMSO-water (1:1 v/v) contained in a vial was kept in equilibrium with a PBS buffer (10 mM, 1 mL, pH 7.2) and the release of Rho-B was monitored by UV-visible spectroscopy at various time intervals, significant release of Rho-B (75.3%) was observed after 7 h. Similarly, the release studies carried out with the anionic fluorophores CF from the CF (0.30 mM) loaded gel of **8** (36.1 mM, 0.25 mL) in DMSO-water (1:1 v/v) indicated a significant release of the fluorophore (95.6 %) into PBS buffer (10 mM, 1 mL, pH 7.2) after 8h (Figure 36 a-d). Being inspired by the results of the entrapment and release of the cationic fluorophore Rho-B and the anionic fluorophore CF, we examined the entrapment and release of the anticancer drug doxorubicin. Interestingly, 92.4% release of the entrapped doxorubicin was observed in 2 h when a doxorubicin (5.17 mM) loaded gel of **8** (36.2 mM) in DMSO-water (1:1, v/v) was kept in equilibrium with PBS buffer (10 mM, 1 mL, pH 7.2) (Figure 33 e-h) making it useful for prospective drug delivery applications. The rate of the release of the drug doxorubicin was much faster in this case compared to the release of the same drug from a drug (0.31 mM) loaded gel of arjunolic acid **7** (4.26 mM) in ethanol- water (3:4 v/v) into PBS buffer at pH 7.2. Thus different triterpenoid systems can be used depending upon ones requirement for effective drug delivery applications.

The terpenoids being functionally rich with several hydroxyl and carboxyl groups innumerable opportunities exist for the generation of terpenoid derivatives depending upon ones design and requirements.[108,109,110,111,112,113,114,115,116,117,118] In this review, we have discussed only the examples of the self-assembly properties of terpenoids without derivatizaiton.

4. Summary and Outlook

In this review, we have discussed how the naturally occurring terpenoids can be utilized as renewable functional nano-entities. The structural diversity of the terpenoids very often with several centres of chirality and several hydroxyl and/or carboxyl groups, in common, have made them very attractive bio-based supramolecular building blocks because these biocompatible frameworks can form diverse nano to micro size architectures like vesicles, fibres, sheets, etc. even without derivatization. The utilization of the self-assemblies have been demonstrated for the entrapment and release of fluorophores including anticancer drug doxorubicin, pollutant capture, generation of hybrid material, etc. Utilization of self-assembled betulinic acid and folic acid conjugate has been demonstrated for selective damage of cancer cells when studied with KG-1A and K562 cancer cells. The basic structures of the terpenoids are amenable to a wide variety of structural modifications opening up the generation of libraries of compounds having different polarity regions and interacting groups. Future studies on the self-assembly of newer terpenoids will help in improved understanding of the structure-property relationships and the development of a green and sustainable world.

4. Acknowledgements

BGB thanks Science and Engineering Research Board (SERB), India (ref. EMR/2016/001123), India Srilanka project (DST/INT/SL/P25/2016), UGC-MRP, UGC-Innovative Project, UGC-SAP and DST-FIST New Delhi and Vidyasagar University for financial support and infrastructural facilities. ACB, NH, SD, CG, SKP and SS thank UGC and SG thanks CSIR for research fellowships.

5. References

1 Hadacek, F. Secondary Metabolites as Plant Traits: Current Assessment and Future Perspectives. *Crit Rev in Plant Sciences* **2002**, 21, 273-322.

2. Hill, R. A. and. Connolly, J. D. Triterpenoids. *Nat. Prod. Rep.,* **2017**, 34, 90-122.

3 (a) Kamm, B. Production of Platform Chemicals and Synthesis Gas from Biomass. *Angew. Chem. Int. Ed.* **2007**, 46, 5056 – 5058. (b) Alonso, D. M.; Bond, J. Q.; Dumesic, J. A. Catalytic conversion of biomass to biofuels. *Green Chem.* **2010**, 12, 1493–1513. (c) Climent, M. J.; Corma, A.; Iborra, S. Converting Carbohydrates to Bulk Chemicals and Fine Chemicals over Heterogeneous Catalysts. *Green Chem.* **2011**, 13, 520–540. (d) Gallezot, P. Conversion of biomass to selected chemical products. *Chem. Soc. Rev.* **2012**, 41, 1538–1558. (e) Kobayashi, H.; Fukuoka, A. Synthesis and utilisation of sugar compounds derived from lignocellulosic biomass. *Green Chem.* **2013**, 15, 1740 - 1763.

4 Brachi, P.; Miccio, F.; Ruoppolo, G.; Miccio, M. Pressurized Steam Torrefaction of Biomass: Focus on Solid, Liquid and Gas Phase Distributions. *Ind. Eng. Chem. Res.* DOI: 10.1021/acs.iecr.7b02845.

5 Anastas, P. T.; Kirchhoff. M. M. Origins, Current Status, and Future Challenges of Green Chemistry. *Acc. Chem. Res.* **2002**, 35, 686–694.

6 Farrán, A.; Cai, C.; Sandoval, M.; Xu, Y.; Liu, J.; Hernáiz, M. J.; Linhardt , R. J. Green Solvents in Carbohydrate Chemistry: From Raw Materials to Fine Chemicals. *Chem. Rev.* **2015**, 115, 6811–6853.

7 Barta, K.; Ford, P. C. Catalytic Conversion of Nonfood Woody Biomass Solids to Organic Liquids. *Acc. Chem. Res.* **2014**, 47, 1503–1512.

8 Lichtenthaler, F. W. Unsaturated O- and N-Heterocycles from Carbohydrate Feed stocks. *Acc. Chem. Res.* **2002**, 35**,** 728-737.

9 Gandini, A.; Lacerda, T. M.; Carvalho, A. J. F.; Trovatti, E. Progress of Polymers from Renewable Resources: Furans, Vegetable Oils, and Polysaccharides. *Chem. Rev.* **2016**, 116, 1637–1669.

10 Besson, M.; Gallezot, P.; Pinel, C. Conversion of biomass into chemicals over metal catalysts. *Chem. Rev.* **2014**, 114, 1827–1870.

11 Zheng, J.J.; Birktoft, Y.; Chen, T.; Wang, R.; Sha, P.E.; Constantinou, S.L.; nell, G.; Mao, C.; Seeman, N.C. From molecular to macroscopic via the rational design of a self-assembled 3D DNA crystal. *Nature* **2009**, 461, 74-77.

12. Grirrane, A.; Corma, A.; Garcia, H. Preparation of symmetric and asymmetric aromatic azo compounds from aromatic amines or nitro compounds using supported gold catalysts. *Nature Protocols* **2010**, 11, 429-438.

13. Peng, G.; Tisch, U.; Adams, O.; Hakim, M.; Shehada, N.; Broza, Y.Y.; Billan, S.; Abdah-Bortnyak, R.; Kuten, A.; Haick, H. Diagnosing lung cancer in exhaled breath using gold nanoparticles. *Nature Nanotech.* **2009**, 4, 669-673.

14. Kim, B.; Han, G.; Toley, B.J.; Kim, C.K.; Rotello, V.M.; Forbes, N.S. Tuning payload delivery in tumour cylindroids using gold nanoparticles. *Nature Nanotech.* **2010**, 5, 465–472.

15 Novo, C.; Funston, A.M.; Mulvaney, P. Direct observation of chemical reactions on single gold nanocrystals using surface plasmon spectroscopy. *Nature Nanotech.* **2008**, 3, 598-602.

16 Alkilany, A.M.; Lohse, S.E.; Murphy, C.J. The Gold Standard: Gold Nanoparticle Libraries To Understand the Nano–Bio Interface. *Acc. Chem. Res.* **2013,** 46, 650–661.

17 Zhang, Y.; Cui, X.; Shi, F.; Deng, Y.; Nano-Gold Catalysis in Fine Chemical Synthesis. *Chem. Rev.* **2012,** 112, 2467-2505.

18 Murphy, C.J.; Gole , A.M.; Stone, J.W.; Sisco, P.N.; Alkilany , A.M.; Goldsmith , E.C.; Baxter, S.C. Gold nanoparticles in biology: beyond toxicity to cellular imaging. *Acc. Chem. Res.* **2008**, 41, 1721 – 1730.

19 Prati, L.; Villa, A. Gold Colloids: From Quasi-Homogeneous to Heterogeneous Catalytic Systems. *Acc. Chem. Res.* 2014, **47**, 855-863.

20 Thomas, K.G.; Kamat, P.V. Chromophore-Functionalized Gold Nanoparticles. *Acc. Chem. Res.* **2003**, 36, 888-898.

21 (a) Seeman, N. C. Nanomaterials based on DNA. *Annu. Rev. Biochem.* **2010**, 79, 65–87. (b) Stulz, E.; Clever, G.; Shionoya, M.; Mao, C. DNA in a modern world. *Chem. Soc. Rev.* **2011**, 40, 5633–5635. (c)

Torring, T.; Voigt, N. V.; Nangreave, J.; Yan, H.; Gothelf, K. V. DNA origami: a quantum leap for self-assembly of complex structures. *Chem. Soc. Rev*. **2011**, 40, 5636–5646.

22 Simmel, S.S.; Nickels P. C.; Liedl, T. Wireframe and Tensegrity DNA Nanostructures. *Acc. Chem. Res*. **2014**, 47, 1691–1699.

23 Yatsunyk, L.A.; Mendoza, O.; Mergny, J.L. "Nano-oddities": Unusual Nucleic Acid Assemblies for DNA-Based Nanostructures and Nanodevices. *Acc. Chem. Res*. **2014**, 47, 1836–1844.

24 Shang, L.; Nienhaus, G. U. In Situ Characterization of Protein Adsorption onto Nanoparticles by Fluorescence Correlation Spectroscopy. *Acc. Chem. Res*. **2017**, 50, 387–395.

25 Seeberger, P.H. The Logic of Automated Glycan Assembly. *Acc. Chem. Res*. **2015**, 48, 1450–1463.

26 Salgado, E. N.; Radford R. J.; Tezcan, F.A. Metal-Directed Protein Self-Assembly. *Acc. Chem. Res*. **2010**, 43, 661–672.

27 SzymaŃski, W.; Yilmaz, D.; Koçer, A.; Feringa, B.L. Bright Ion Channels and Lipid Bilayers. *Acc. Chem. Res*. **2013**, 46, 2910–2923.

28 (a) Eschenmoser, A.; Ruzicka, L.; Jeger, O.; Arigoni, D. Zur Kenntnis der Triterpene. 190. Mitteilung. Eine stereochemische Interpretation der biogenetischen Isoprenregel bei den Triterpenen. *Helv. Chim. Acta* **1955**, 38, 1890-1904. (b) Eschenmoser, A.; Arigoni, D. Revisited after 50 Years: The 'Stereochemical Interpretation of the Biogenetic Isoprene Rule for the Triterpenes. *Helv. Chim. Acta*. **2005**, 88, 3011–3050.

29 Bag, B.G.; Garai, C.; Majumdar, R.; Laguerre, M. Natural triterpenoids as renewable nanos. *Struct. Chem*. **2012**, 23, 393-398.

30 Bag, B.G.; Barai, A.C.; Hasan, S.N; Das, S.; Garai, C.; Ghorai, S.; Panja, S. K. "Terpenoids as Renewable Nano-Sized Building Blocks" under review.

31 Chang, G.; Guida, W.C.; Still, W.C. An internal-coordinate Monte Carlo method for searching conformational space. *J. Am. Chem. Soc.* **1989**, 111, 4379-4386.

32 Saunders, M.; Houk, K.N.; Wu, Y.D.; Still, W.C.; Lipton, M.; Chang, G.; Guida, W.C. Conformations of cycloheptadecane: A comparison of methods for conformational searching. *J. Am. Chem. Soc.* **1990**, 112, 1419-1427.

33 (a) Sorrenti, A.; Illa, O.; Ortuno, R. M. Amphiphiles in aqueous solution: well beyond a soap bubble. *Chem. Soc. Re.* **2013**, 42, 8200-8219. (b) Hauser, C. A. E.; Zhang, S. Nanotechnology: Peptides as biological semiconductors. *Nature* **2010**, 468, 516-517. (c) Amdursky, N.; Molotskii, M.; Gazit, E.; Rosenman, G. Elementary Building Blocks of Self-Assembled Peptide Nanotubes. *J. Am. Chem. Soc.* **2010**, 132, 15632-15636.

34 (a) Busseron, E.; Ruff, Y.; Moulin, E.; Giuseppone, N. Supramolecular self-assemblies as functional nanomaterials. *Nanoscale* **2013**, 5, 7098-7140. (b) Yao, H. B.; Fang, H. Y.; Wang, X. H.; Yu, S. H. Hierarchical assembly of micro-nano-building blocks: bio-inspired rigid structural functional materials. *Chem. Soc. Rev.* **2011**, 40, 3764-3785. (c) Grzelczak, M.; Vermant, J.; Furst, E. M.; Liz-Marza´n, L. M. Directed Self-Assembly of Nanoparticles. *ACS Nano* **2010**, 4, 3591-3605.

35 (a) Carretti, E.; Bonini, M.; Dei, L.; Berrie, B.H.; Angelova, L.V.; Baglioni P.; Weiss, R.G. New Frontiers in Materials Science for Art Conservation: Responsive Gels and Beyond. *Acc. Chem. Res.* **2010**, 43, 751-760. (b) Babu, S.S.; Praveen, V.K.; Ajayaghosh, A. Functional π-Gelators and Their Applications. *Chem. Rev*. **2014**, 114, 1973-2129. (c) Suzuki M.; Hanabusa, K. Structure–activity effects in peptide self-assembly and gelation – Dendritic versus linear architectures. *Chem. Soc. Rev*. **2009**, 38, 967-975. (d) George M.; Weiss, R.G. Molecular Organogels. Soft Matter Comprised of Low-Molecular-Mass Organic Gelators and Organic Liquids. *Acc. Chem. Res*. **2006**, 39, 489-497. (e) Weiss, R.G.; Terech, P. Molecular Gels: Materials with Self-Assembled Fibrillar Networks; Springer: Dordrecht **2006**.

36 (a) Ajayaghosh, A.; Praveen, V. K. π-Organogels of Self-Assembled p-Phenylenevinylenes: Soft Materials with Distinct Size, Shape, and Functions. *Acc. Chem. Res.* **2007**, 40, 644-656. (b) Ajayaghosh, A.; Varghese, R.; Mahesh, S.; Praveen, V. K. From Vesicles to Helical Nanotubes: A Sergeant-and-Soldiers Effect in the Self-Assembly of Oligo. (p-phenyleneethynylene) *Angew. Chem*. **2006**, 118, 7893-7896. *Angew. Chem. Int. Ed*. **2006**, 45, 7729-7732. (c) Shimizu, T.; Masuda, M.; Minamikawa, H. Evolution of Nano- to Microsized Spherical Assemblies of a Short Oligo(p-phenyleneethynylene) into Superstructured Organogels. *Chem. Rev*. **2005**, 105, 1401-1444. (d) Ajayaghosh, A.; Varghese, R.; Mahesh, S.; Praveen, V. K. Organogels as scaffolds for excitation energy transfer and light harvesting. *Angew. Chem.* **2006**, 118, 3339-3342. *Angew. Chem. Int. Ed*. **2006**, 45, 3261-3264.

37 Datta, S.; Bhattacharya, S. Multifarious facets of sugar-derived molecular gels: molecular features, mechanisms of self-assembly and emerging applications. *Chem. Soc. Rev.* **2015**, 44, 5596-5637.

38 (a) Das, D.; Kar, T.; Das, P. K. Gel-nanocomposites: materials with promising applications. *Soft Matter* **2012**, 8, 2348 – 2365. (b) Koley, P.; Pramanik, A. Nanostructures from Single Amino Acid-Based Molecules: Stability, Fibrillation, Encapsulation, and Fabrication of Silver Nanoparticles. *Adv. Funct. Mater*. **2011**, 21, 4126 – 4136.

39 (a) Delample, M.; J´erˆome, F.; Barrault, J.; Douliez, J. P. Self-assembly and emulsions of oleic acid–oleate mixtures in glycerol. *Green Chem.* **2011**, 13, 64-68. (b) Novales, B.; Navailles, L.; Axelos, M.; Nallet, F.; Douliez, J. P. Self-Assembly of Fatty Acids and Hydroxyl Derivative Salts. *Langmuir* **2008**, 24, 62–68. (c) Douliez, J. P. Self-Assembly of Hollow Cones in a Bola-amphiphile/Hexadiamine

Salt Solution. *J. Am. Chem. Soc.* **2005**, 127, 15694–15695.

40 (a) Baccile, N.; Nassif, N.; Malfatti, L.; Van Bogaert, I.N.A.; Soetaert, W.; Pehau-Arnaudet, G.; Babonneau, F. Sophorolipids: a yeast-derived glycolipid as greener structure directing agents for self-assembled nanomaterials. *Green Chem.* **2010**, 12, 1564–1567. (b) Zhou, S.; Xu, C.; Wang, J.; Gao, W.; khverdiyeva, R.; Shah, V.; Gross, R. Supramolecular Assemblies of a Naturally Derived Sophorolipid. *Langmuir* **2004**, 20, 7926-7932.

41 Vemula, P. K.;John, G. Crops: A Green Approach toward Self-Assembled Soft Materials. *Acc. Chem. Res.* **2008**, 41**,** 769–782.

42 Sato, T.; Yoshida, S.; Hoshino, H.; Tanno, M.; Nakajima, M.; Hoshino, T. Sesquarterpenes (C35 Terpenes) Biosynthesized via the Cyclization of a Linear C35 Isoprenoid by a Tetraprenyl-β-curcumene Synthase and a Tetraprenyl-β-curcumene Cyclase: Identification of a New Terpene Cyclase. *J. Am. Chem. Soc.* **2011**, 133, 9734–9737

43 Bag, B.G.; Majumdar, R. Self–assembly of renewable nano–sized triterpenoids. *Chem. Rec.* **2017**, 17, DOI: 10.1002/tcr.201600123.

44 'Diterpenoids: Types, Functions and Research, Brandon Jones ed., Nova Science Publishers **2017**.

45 Bag, B.G.; Barai, A.C.; Wijesekera, K.; Kittakoop, P. First Vesicular Self-Assembly of Crotocembraneic Acid, a Nano-Sized Fourteen Membered Macrocyclic Diterpenic Acid. *Chemistry Select* **2017**, 2, 4969-4973.

46 Youngsa-ad, W.; Ngamrojanavanich, N.; Mahidol, C.; Ruchirawat, S.; Prawat, H.; Kittakoop, P. Diterpenoids from the Roots of Croton oblongifolius. *Planta Med.* **2007**, 73, 1491-4.

47 Roengsumran, S.; Achayindee, S.; Petsom, A.; Pudhom, K.; Singtothong, P.; Surachetapan, C.; Vilaivan, T. Unprecedented Oxylipins from the Marine Green Alga Acrosiphonia coalita. *J.Nat.Prod.* **1998**, 61, 652-654.

48 Antonietti, M.; Foerster, S. Vesicles and Liposomes: A Self-Assembly Principle Beyond Lipids. *Adv. Mater***. 2003**, 15, 1323-1333.

49 Fulda, S. Betulinic Acid for Cancer Treatment and Prevention. *Int. J. Mol. Sci.* **2008**, 9, 1096 – 1107.

50 Pisha, E.; Chai, H.; Lee, I.S.; Chagwedera, T.E.; Farnsworth, N.R.; Cordell, G.A.; Beecher, C.W.W.; Fong, H.H.S.; Kinghorn, A.D.; Brown, D.M.; Wani, M. C.; Wall, M. E.; Hieken, T.J.; Das Gupta, T.K.; Pezzuto, J. Discovery of betulinic acid as a selective inhibitor of human melanoma that functions by induction of apoptosis. M. *Nat. Med.* **1995,** 1, 1046-1051.

51 Schmidt, M.L.; Kuzmanoff, K.L.; Ling-Indeck, L.; Pezzuto, J.M. Betulinic acid induces apoptosis in human neuroblastoma cell lines. *Eur. J. Cancer* **1997,** 33, 2007-2010.

52 Genet, C.; Strehle, A.; Schmidt, C.; Boudjelal, G.; Lobstein, A.; Schoonjans, K.; Souchet, M.; Auwerx, J.; Saladin, R.; Wagner, A. Structure–Activity Relationship Study of Betulinic Acid, A Novel and Selective TGR5 Agonist, and Its Synthetic Derivatives: Potential Impact in Diabetes. *J. Med. Chem.* **2010**, 53, 178-190.

53 Bag, B.G.; Dash, S.S. First self-assembly study of betulinic acid, a renewable nano-sized, 6-6-6-6-5 pentacyclic monohydroxy triterpenic acid. *Nanoscale* **2011**, 3, 4564-4566.

54 Ali, A.; Kamra, M.; Bhan, A.; Mandal, S. S.; Bhattacharya, S. New Fe(III) and Co(II) salen complexes with pendant distamycins: selective targeting of cancer cells by DNA damage and mitochondrial pathways. *Dalton Trans.* **2016**, 45, 9345–9353.

55 Dash, S. K.; Dash, S. S.; Chattopadhyay, S.; Ghosh, T.; Tripathy, S.; Kar Mahapatra, S.; Bag, B. G.; Das D.; Roy, S. Folate decorated delivery of self assembled betulinic acid nano fibers: a biocompatible anti-leukemic therapy. *RSC Adv.* **2015**, 5, 24144–24157.

56 Dash, S.K.; Chattopadhyay, S.; Dash, S. S.; Tripathy, S.; Das, B.; Mahapatra, S. K.; Bag, B.G.; Karmakar, P.; Roy, S. Self assembled nano fibers of betulinic acid: A selective inducer for ROS/TNF-alpha pathway mediated leukemic cell death. *Bioorg. Chem.* **2015**, 63, 85-100.

57 Dash, S. K.; Chattopadhyay, S.; Tripathy, S.; Dash, S. S.; Das, B.; Mandal, D.; Mahapatra, S.D.; Bag, B. G.; Roy, S. Self-assembled betulinic acid augments immunomodulatory activity associates with IgG response. *Biomed Pharmacother* **2015**, 75, 205-217.

58 Kislitsyn, A. N. Lignin. Structural organisation and fractal properties. *Khimiya Drevesiny* **1994**, 3, 3.

59 Tolstikov, G. A.; Flekhter, O. B; .É. É. Shul'ts et al. *Khimiya v Interesakh Ustoichivogo Razvitiya* **2005**, 13, 1.

60 Bag, B.G.; Dash, S.S. Hierarchical Self-Assembly of a Renewable Nanosized Pentacyclic Dihydroxy-triterpenoid Betulin Yielding Flower-Like Architectures. *Langmuir* **2015**, 31, 13664-13672.

61 Moitra, P.; Kumar, K.; Kondaiah, P.; Bhattacharya, S. Efficacious Anticancer Drug Delivery Mediated by a pH-Sensitive Self-Assembly of a Conserved Tripeptide Derived from Tyrosine Kinase NGF Receptor. *Angew. Chem., Int. Ed.* **2014**, 53, 1113-1117.

62 Baral, A.; Roy, S.; Dehsorkhi, A.; Hamley, I. W.; Mohapatra, S.; Ghosh, S.; Banerjee, A. Assembly of an Injectable Noncytotoxic Peptide-Based Hydrogelator for Sustained Release of Drugs. *Langmuir* **2014**, 30, 929–936.

63 Kalafatovic, D.;. Nobis, M; Javid, N.; Frederix, P. W. J. M.; Anderson, K.; Saunders, B.R.; Ulijn, R. V. MMP-9 triggered micelle-to-fibre transitions for slow release of doxorubicin. *Biomater. Sci.* **2015**, 3, 246-249.

64 Tian, B.; Tao, X.; Ren, T.; Weng, Y.; Lin, X.; Zhang, Y.; Tang, X. Polypeptide-based vesicles: formation,

properties and application for drug delivery. *J. Mater. Chem.* **2012**, 22**,** 17404-17414.

65 Mittal, A.; Mittal, J.; Malviya, A.; Kaur, D.; Gupta, V. K. Adsorption of hazardous dye crystal violet from wastewater by waste materials. *J. Colloid Interface Sci.* **2010**, 343, 463-473.

66 Bag, B.G.; Paul, K. Vesicular and Fibrillar Gels by Self-Assembly of Nanosized Oleanolic Acid. *Asian J. Org. Chem.* **2012**, 1, 150-154.

67 Banik, R.M.; Pandey, D.K. Optimizing conditions for oleanolic acid extraction from Lantana camara roots using response surface methodology. *Ind. Crop. Prod.* **2008**, 27, 241 – 243.

68 Shyu, M. H.; Kao, T. C.; Yen, G. C. Oleanolic Acid and Ursolic Acid Induce Apoptosis in HuH7 Human Hepatocellular Carcinoma Cells through a Mitochondrial-Dependent Pathway and Downregulation of XIAP. *J. Agric. Food Chem.* **2010**, 58, 6110–6118.

69 Yang, M.; Wang, W.; Yuan, F.; Zhang, X.; Li, J.; Liang, F.; He, B.; Minch, B.; Wegner, G. Soft Vesicles Formed by Diblock Codendrimers of Poly(benzyl ether) and Poly(methallyl dichloride) *J. Am. Chem. Soc.* **2005**, 127, 15107-15111.

70 Nystro¨m, A.M.; Xu, Z.; Xu, J.; Taylor, S.; Nittis, T.; Stewart, S.A.; Leonard, J.; Wooley, K.L. SCKs as nanoparticle carriers of doxorubicin: investigation of core composition on the loading, release and cytotoxicity profiles. *Chem. Commun.* **2008**, 3579 – 3581.

71 Gillies E. R.; Fre´chet, J. M. pH-Responsive Copolymer Assemblies for Controlled Release of Doxorubicin. J. *Bioconjugate Chem.* **2005**, 16*,* 361–368.

72 Soppimath, K. S.; Liu, L.H.; Seow, W. Y.; Liu, S. Q.; Powell, R.; Chan P.; Yang, Y. Y. Multifunctional Core/Shell Nanoparticles Self-Assembled from pH-Induced Thermosensitive Polymers for Targeted Intracellular Anticancer Drug Delivery. *Adv. Funct. Mater.* **2007**, 17, 355–362.

73 (a) Barenholz, Y. Emulsions, Foams, and Suspensions: Fundamentals and Applications. *Colloid Interface Sci.* **2001**, 6, 66–77. (b) Malam, Y.; Loizidou, M.; Seifalian, A.M. Liposomes and nanoparticles: nanosized vehicles for drug delivery in cancer. *Trends Pharmacol. Sci.* **2009**, 30, 592-599. (c) Schroeder, A.; Turjeman, K.; Schroeder, J.E.; Leibergall, M.; Barenholz, Y. Using liposomes to target infection and inflammation induced by foreign body injuries or medical implants. *Exp. Opin. Drug Delivery* **2010**, 7, 1175–1189. (d) Allen, T.M.; Cullis, P.R. Drug delivery systems: entering the mainstream. *Science* **2004**, 303, 1818–1822. (e) Allen, T.M. Ligand-targeted therapeutics in anticancer therapy. *Nat. Rev. Cancer* **2002**, 2, 750–763. (f) Lasic, D.D.; Templeton, N.S. Liposomes in gene therapy. *Adv. Drug Delivery Rev.* **1996**, 20, 221–266. (g) Peterca, M.; Percec, V.; Leowanawat, P.; Bertin A. Predicting the Size and Properties of Dendrimersomes from the Lamellar Structure of Their Amphiphilic Janus Dendrimers. *J. Am. Chem. Soc.* **2011**, 133, 20507–20520.

74 Silva, J. A.; Silva, A. G.; Alves, A. S.; Reis, R.; Nascimento, C. C.; Dir´e G. F.; Barreto, A. S. Plumeria rubra (Apocynaceae): A good source of ursolic acid. *J. Med. Plants Res.* **2013**, 7, 892–896.

74. Lu, J.; Wu, X.; Liu, L.; Chen H.; Liang, Y. First Organogelation Study of Ursolic Acid, a Natural Ursane Triterpenoid. *Chem. Lett.*, **2016**, 45, 860–862.

76 Es-saady, D.; Najid, A.; Simon, A.; Chulia A. J.; Delage, C. Cytotoxic Triterpenoids from Erica andevalensis. *Lyon Pharm.* **1994,** 45, 399–404.

77 Lee, H. Y.; Chung, H. Y.; Kim, K. H.; Lee J. J.; Kim, A. W. Molecular and cellular biology of prostate cancer. *J. Cancer Res. Clin. Oncol.* **1994**, 120, 513–518.

78 Umehara, K.; Takagi, R.; Kuroyanagi, M.; Ueno, A.; Taki, T. Y. J. *Chen, Chem. Bull.* **1992**, 40, 401–405.

79 Cordero, C. M.; Reyes, M.; Ayuso M. J.; Toro, M. V. Z. Cytotoxic Triterpenoids from Erica andevalensis. *Naturforsch.* **2001**, 56, 45–48.

80 Li, J.; Guo W. J.; Yang, Q. Y. Effects of ursolic acid and oleanolic acid on human colon carcinoma cell line HCT15. *World J. Gastroenterol.* **2002**, 8, 493–495.

81 Lauthier, F.; Taillet, L.; Trouillas, P.; Delage, C.; Simon, A. Ursolic acid triggers calcium-dependent apoptosis in human Daudi cells. *Anticancer Drugs*, **2000,** 11, 737–745.

82 Cha, H.; Park, M. T.; Chung, H. Y.; Kim, N. D.; Sato, H.; Seiki, M.; Kim, K. W. . Role of ursolic acid chalcone, a synthetic analogue of ursolic acid, in inhibiting the properties of CD133+ sphere-forming cells in liver stem cells. *Oncogene*, **1998**, 16, 771–778.

83 Bag, B. G.; Das, S.; Hasan S. N.; Barai A. C. Nanoarchitectures by hierarchical self-assembly of ursolic acid: entrapment and release of fluorophores including anticancer drug doxorubicin. *RSC Adv.* **2017**, 7, 18136.

84 (a) Skeel R. T.; Khleif, S. N. *Handbook of Cancer Chemotherapy* **2011**, 8, 1–15. (b) Skeel R. T.; Khleif, S. N. *Handbook of Cancer Chemotherapy* **2011**, 8, 45–62.

85 Tian, B.; Tao, X.; Ren, T.; Weng, Y.; Lin, X.; Zhang Y.; Tang, X. Synthesis and properties of 3,4,5-trinitropyrazole-1-ol and its energetic salts. *J. Mater. Chem.* **2012**, 22, 17404.

86 Moitra, P.; Kumar, K.; Kondaiah P.; Bhattacharya, S. Efficacious Anticancer Drug Delivery Mediated by a pH-Sensitive Self-Assembly of a Conserved Tripeptide Derived from Tyrosine Kinase NGF Recepto. *Angew. Chem., Int. Ed.* **2014**, 53, 1113.

87 Ali, A.; Kamra, M.; Bhan, A.; Mandal S. S.; Bhattacharya, S. New Fe(III) and Co(II) salen complexes with pendant distamycins: selective targeting of cancer cells by DNA damage and mitochondrial pathways. *Dalton Trans.* **2016**, 45, 9345–9353.

88 Nakahara, Y.; Okazaki Y.; Kimura, K. Self-assembling phenomena of benzo-18-crown-6/crowned-spirobenzopyran copolymers in aqueous solution and controlled release of entrapped organic dyes using external stimuli. *Soft Matter* **2012**, **8**, 3192.

89 Thota, C. K.; Yadav N.; Chauhan, V. S. A novel highly stable and injectable hydrogel based on a conformationally restricted ultrashort bn peptide. *Sci. Rep*. **2016**, 6, 31167.

90 Luo, Z.; Li, Y.; Wang B.; Jiang, J. Synthesis and Electroluminescence of a Conjugated Polymer with Thermally Activated Delayed Fluorescence. *Macromolecules* **2016**, 49, 6084–6094.

91 Baral, A.; Roy, S.; Dehsorkhi, A.; Haamlay, I. W.; Mohapatra, S.; Ghosh, S.; Banerjee, A. Assembly of an Injectable Noncytotoxic Peptide-Based Hydrogelator for Sustained Release of Drugs. *Langmuir* **2014**, 30, 929–936.

92 Kim, D.H.; Hong, S.W.; Kim, B.T.; Bae, E.A.; Park H.Y.; Han, M.J. Biotransformation of glycyrrhizin by human intestinal bacteria and its relation to biological activities. *Arch. Pharm. Res*. **2000**, 23, 172–177.

93 Kao, T.C.; Shyu, M.H.; Yen G.C. Glycyrrhizic acid and 18beta-glycyrrhetinic acid inhibit inflammation via PI3K/Akt/GSK3beta signaling and glucocorticoid receptor activation. *J. Agric. Food Chem*. **2010**, 58, 8623–8629.

94 Ikeda, T.; Yokomizo, K.; Okawa, M.; Tsuchihashi, R.; Kinjo, J.; Nohara T.; Uyeda, M. Anti-herpes Virus Type 1 Activity of Oleanane-Type Triterpenoids. *Biol. Pharm. Bull.* **2005**, 28, 1779–1781.

95 Bag, B. G.; Majumdar, R. Self-assembly of a renewable nano-sized triterpenoid 18b-glycyrrhetinic Acid. *RSC Adv*. **2012**, 2, 8623 –8626.

96 (a) Langer, D.; Wicher, B.; Szczołko, W.; Gdaniec, M.; Tykarska, E. Acta E transforms from Structure Reports Online to Crystallographic Communications. *Acta Cryst.* **2016**. B72, 584-592. (b) Tykarska, E.; Gdaniec, M. Solid-state supramolecular architecture of carben-oxolone - comparative studies with glycyrrhetinic and glycyrrhizic acids. *Acta Cryst*. **2015,** B71, 25-33.

97 Rengaraj, S.; Venkataraj, S.; Jee, S.H.; Kim, Y.; Tai, C.W.; Repo, E.; Koistinen, A.; Ferancova A.; Sillanp, M. Cauliflower-like CdS Microspheres Composed of Nanocrystals and Their Physicochemical Properties. *Langmuir* **2011**, 27, 352–358.

98 Ock, K.S.; Ganbold, E.O.; Jeong, S.; Seo J.H.; Joo, S.W. CdS Nanoparticles as Efficient Fluorescence Resonance Energy Transfer Donors for Various Organic Dyes in an Aqueous Solution. *Bull. Korean Chem. Soc.* **2011**, 32*,* 3610–3613.

99 Wu, D.; Ge, X.; Zhang, Z.; Wang M.; Zhang, S. Novel One-Step Route for Synthesizing CdS/Polystyrene Nanocomposite Hollow Spheres. *Langmuir* **2004**, 20, 5192–5195.

100 Bag, B.G.; Dey, P.P.; Dinda, S.K.; Sheldrick, W.S.; Oppel, I.M. A simple route for renewable nano-sized arjunolic and asiatic acids and self-assembly of arjunabromolactone. *Beil. J. Org. Chem*. **2008**, 4, 1-5.

101 Bag, B. G.; Majumdar, R. Vesicular self-assembly of a natural triterpenoid arjunolic acid in aqueous medium: study of entrapment properties and in situ generation of gel–gold nanoparticle hybrid material. *RSC Adv*. **2014**, 4, 53327–53334.

102 Saleesh Kumar, N. S.; Varghese, S.; Narayan G.; Das, S. Hierarchical Self-Assembly of Donor–Acceptor-Substituted Butadiene Amphiphiles into Photoresponsive Vesicles and Gels. *Angew. Chem., Int. Ed*. **2006**, 45, 6317–6321.

103 Tian, B.; Tao, X.; Ren, T.; Weng, Y.; Lin, X.; Zhang Y.; Tang, X. Polypeptide-based vesicles: formation, properties and application for drug delivery. *J. Mater. Chem.* **2012**, 22, 17404-17414.

104 (a) Misra, S. K.; Kondaiah, P.; Bhattacharya S.; Rao, C. N. R. Graphene as a nanocarrier for tamoxifen induces apoptosis in transformed cancer cell lines of different origins. *Small*, **2012**, 8, 131-143. (b) Misra, S. K.; Moitra, P.; Chhikara, B. S.; Kondaiah P.; Bhattacharya, S. *J. Mater. Chem.* **2012**, 22, 7985-7998.

105 Majumdar, R., Tantayanon, S., Bag, B. G., A Novel Trihybrid Material Based on Renewables: An Efficient Recyclable Heterogeneous Catalyst for C-C Coupling and Reduction Reactions. *Chem. Asian J.* **2016**, 11,2406–2414

106 Pongpamorn, P.; Wan-erlor, S.; Ruchirawat, S.; Thasana, N. Lycoclavatumide and 8□,11□-dihydroxylycopodine, a new fawcettimine and lycopodine-type alkaloid from Lycopodium clavatum. *Tetrahedron* **2016**, 72, 7065-7069.

107 Bag, B.G.; Hasan, S.N.; Pongpamorn, P.; Thasana, N. First Hierarchical Self-Assembly of a Seco-Triterpenoid □-Onocerin Yielding Supramolecular Architectures. *ChemistrySelect* **2017**, 2, 6650-6657.

108 Bag, B.G.; Dash, S.S. Self-assembly of sodium and potassium betulinates into hydro- and organo-gels: entrapment and removal studies of fluorophores and synthesis of gel–gold nanoparticle hybrid materials. *RSC Adv*. **2016**, 6, 17290-17296.

109 Bag, B.G.; Dinda, S.K.; Dey, P.P.; Mallia, V.A.; Weiss, R.G. Self-Assembly of Esters of Arjunolic Acid into Fibrous Networks and the Properties of their Organogels. *Langmuir* **2009**, 25, 8663-8671.

110 Bag, B. G.; Majumdar, R.; Dinda, S. K.; Dey, P. P.; Maity, G. C.; Mallia, V. A.; Weiss, R. G. Self-Assembly of Ketals of Arjunolic Acid into Vesicles and Fibers Yielding Gel-Like Dispersions. *Langmuir* **2013**, 29, 1766–1778.

111 Bag, B.G.; Maity, G.C.; Pramanik, S.R. Arjunolic Acid in Molecular Recognition: First Synthesis and Cation Binding Studies of a novel Arjuna-18-crown-6. *Supramol. Chem*. **2005**, 17*,* 383-385.

112 Bag, B. G.; Maity, G. C.; Dinda, S. K. Donor-Acceptor Interaction Promoted Gelation: Visual Observation of Color Change. *Organic Letters* **2006**, 8, 5457-5460.

113 Bag, B. G.; Dinda, S.K. Arjunolic acid: A renewable template in supramolecular chemistry and

nanoscience. *Pure & Appl. Chem.* **2007**, 79, 2031-2038.

114 Bhargavi, R.; Nair, G.; Prasad, S. K.; Majumdar, R.; Bag, B. G. A charge transfer complex nematic liquid crystalline gel with high electrical conductivity. *J. Appl. Phys*. **2014**, 116, 154902.

115 Gao, Y.; Hao, J.; Wu, J.; Zhang, X.; Hu, J.; Ju, Y. Supramolecular helical nanofibers assembled from a pyridinium-functionalized methyl glycyrrhetate amphiphile. *Nanoscale* **2015**, 7, 13568- 13575.

116 Gao, Y.; Hao, J.; Wu, J.; Zhang, X.; Hu, J.; Ju, Y. Solvent-Directed Assembly of a Pyridinium-Tailored Methyl Oleanolate Amphiphile: Stepwise Growth of Microrods and Nanofibers. *Langmuir* **2016**, 32, 1685- 1692.

117 Lu, J.; Hu, J.; Song, Y.; Ju, Y. A New Dual-Responsive Organogel Based on Uracil-Appended Glycyrrhetinic Acid. *Org. Lett*. **2011**, 13, 3372-3375.

118 Lu, J.; Hu, J.; Liu, C.; Gao H.; Ju, Y. Water-induced gel formation of an oleanlic acid–adenine conjugate and the effects of uracil derivative on the gel stability. *Soft Matter* **2012**, 8, 9576-9580.